


Review

PET Imaging of the Neuropeptide Y System: A Systematic Review

Inês C. F. Fonseca^{1,2,3}, Miguel Castelo-Branco^{1,3,4}, Cláudia Cavadas^{2,5,6} and Antero J. Abrunhosa^{1,3,*} 

¹ CIBIT/ICNAS—Institute for Nuclear Sciences Applied to Health, University of Coimbra, 3000-548 Coimbra, Portugal; inesfonseca@icnas.uc.pt (I.C.F.F.); mcbranco@fmed.uc.pt (M.C.-B.)

² Faculty of Pharmacy, University of Coimbra, 3000-548 Coimbra, Portugal; ccavadas@ci.uc.pt

³ ICNAS Pharma Unipessoal, Lda, Ed. ICNAS, Pólo das Ciências da Saúde, University of Coimbra, 3000-548 Coimbra, Portugal

⁴ Faculty of Medicine, University of Coimbra, 3000-548 Coimbra, Portugal

⁵ CNC—Center for Neuroscience and Cell Biology, University of Coimbra, 3004-504 Coimbra, Portugal

⁶ CIBB—Centre for Innovative Biomedicine and Biotechnology, University of Coimbra, 3004-531 Coimbra, Portugal

* Correspondence: antero@pet.uc.pt

Abstract: Neuropeptide Y (NPY) is a vastly studied biological peptide with numerous physiological functions that activate the NPY receptor family (Y₁, Y₂, Y₄ and Y₅). Moreover, these receptors are correlated with the pathophysiology of several diseases such as feeding disorders, anxiety, metabolic diseases, neurodegenerative diseases, some types of cancers and others. In order to deepen the knowledge of NPY receptors' functions and molecular mechanisms, neuroimaging techniques such as positron emission tomography (PET) have been used. The development of new radiotracers for the different NPY receptors and their subsequent PET studies have led to significant insights into molecular mechanisms involving NPY receptors. This article provides a systematic review of the imaging biomarkers that have been developed as PET tracers in order to study the NPY receptor family.

Keywords: neuropeptide Y; positron emission tomography; neuroimaging; PET radiotracers; NPY receptors



Citation: Fonseca, I.C.F.;

Castelo-Branco, M.; Cavadas, C.; Abrunhosa, A.J. PET Imaging of the Neuropeptide Y System: A Systematic Review. *Molecules* **2022**, *27*, 3726. <https://doi.org/10.3390/molecules27123726>

Academic Editors: Mauricio Morais and Péter Kele

Received: 2 May 2022

Accepted: 5 June 2022

Published: 9 June 2022

Publisher's Note: MDPI stays neutral with regard to jurisdictional claims in published maps and institutional affiliations.



Copyright: © 2022 by the authors. Licensee MDPI, Basel, Switzerland. This article is an open access article distributed under the terms and conditions of the Creative Commons Attribution (CC BY) license (<https://creativecommons.org/licenses/by/4.0/>).

1. Introduction

Molecular imaging has been of immense value to the field of brain research, as the inaccessibility of the brain represents one of the greatest obstacles to central nervous system (CNS) studies [1]. Non-invasive imaging technology has not only played a major role in the discovery and development of CNS drugs but it has also become a prominent approach to the study and clarification of diverse neurological pathways. The uniqueness of the CNS field lies in the existence of its many potential drug targets; however, only a few are being exploited by current CNS therapeutics [2]. CNS diseases are highly heterogeneous, which complicates the elucidation and research of their physiology and can lead to failure in the development of a new potential drug.

The potential of using imaging to optimize CNS drugs' discovery and development relies on various imaging techniques such as computerized tomography (CT), magnetic resonance imaging (MRI), single photon emission computed tomography (SPECT), positron emission tomography (PET) and others [3–5]. The main characteristics of these imaging techniques are summarized in Table 1.

The PET imaging technique uses the distinct decay characteristics of low-dose, high specific activity, short half-life positron-emitting radionuclides. These radionuclides (e.g., ¹¹C, ¹³N, ¹⁸F, ⁶⁸Ga and ⁶⁴Cu), which are usually produced in a cyclotron, are involved in the design and production of radiolabeled tracers that are expected to interact selectively with the target of interest, allowing the in vivo tracing of biochemical processes. PET is

an extremely sensitive technique as it allows radioligands to be detected at picomolar to femtomolar levels. Concerning this and the fact that the positron emitting radioisotopes decay with a reasonably short half-life (e.g., 20 min for ^{11}C and 110 min for ^{18}F), it becomes possible to administer high doses so as to provide a strong imaging signal without producing the long-term health risks that are related to ionizing radiation. Hence, PET allows the quantitative mapping of the spatial distribution of the radiolabeled tracers in living animal species and in living humans [2–12]. Hereby, brain positron emission tomography has led to new findings and changes to the standard concepts in neuroscience; namely in cerebrovascular diseases, movement disorders, dementia, epilepsy, schizophrenia, addiction, depression, anxiety and cerebral tumors [13].

Table 1. Properties and characteristics of the following imaging modalities: CT, MRI, SPECT and PET.

Modality	Characteristics	Advantages	Limitations
CT	<ul style="list-style-type: none"> ■ X-rays ■ Spatial resolution: 0.5 mm 	<ul style="list-style-type: none"> ■ Scanning is fast, painless and non-invasive ■ High spatial resolution ■ Ability to image bone, soft tissue, and blood vessels all at the same time 	<ul style="list-style-type: none"> ■ Ionizing radiation ■ Requires contrast agent ■ Radiation tissue nonspecificity
MRI	<ul style="list-style-type: none"> ■ Spatial resolution: 1 mm 	<ul style="list-style-type: none"> ■ Non-invasive ■ High spatial resolution and soft tissue contrast ■ Lack of ionizing radiation 	<ul style="list-style-type: none"> ■ Low sensitivity ■ Lack of chemical specificity ■ High cost
SPECT	<ul style="list-style-type: none"> ■ Radionuclides (^{123}I, $^{99\text{m}}\text{Tc}$, ^{111}In, ^{67}Ga) ■ Spatial resolution: 6 mm 	<ul style="list-style-type: none"> ■ SPECT images can provide information on physiological and physiopathological processes at a molecular level ■ Non-invasive 	<ul style="list-style-type: none"> ■ Its images are less sensitive and less detailed than PET images ■ Less expensive than PET
PET	<ul style="list-style-type: none"> ■ Radionuclides (^{11}C, ^{13}N, ^{18}F, ^{68}Ga, ^{64}Cu) ■ Spatial resolution: 4 mm 	<ul style="list-style-type: none"> ■ PET images provide physiological and detailed metabolic information ■ Better spatial resolution and higher sensitivity than SPECT ■ Non-invasive 	<ul style="list-style-type: none"> ■ Cyclotron needed ■ High cost

Neuropeptide Y (NPY) is one of the most abundant neuropeptides in the mammalian brain. It is known to participate in essential physiological functions in humans and has been correlated with the pathophysiology of several diseases such as feeding disorders, anxiety, metabolic diseases, neurodegenerative diseases, several types of cancer and others [14–19]. However, despite all of the research around this topic, the neurological pathways that are related to NPY are not quite clearly understood yet. As such, PET imaging emerges as a powerful technique that may be used to study the neuromolecular mechanisms of this neuropeptide.

2. Methodology

The present research was conducted through the utilization of the PubMed, Web of Science and Google Scholar databases (accessed between March 2020 and February 2022), using the following both as text and as MeSH terms: “Neuropeptide Y”, “NPY”, “NPY receptors”, “PET”, “PET imaging” and “NPY PET imaging”. Only articles in English were reviewed. The systematic literature research process included a total of 194 articles. According to the PRISMA flowchart, after duplicate removal, 113 articles have been considered, fully read, analyzed and extensively described according to their title and abstract [20]. Other relevant articles were also checked after they had been found in the references of the articles that were originally included in the retrieved literature.

3. Overview of Neuropeptide Y Family and Receptors

Neuropeptide Y (NPY) is a remarkably conserved 36-amino-acid peptide, being one of the most abundant peptides in the central nervous system of mammals [21,22]. NPY is structurally similar to peptide YY (PYY) and pancreatic peptide (PP) [23]. These three peptides constitute a family of regulatory peptides and they share a common hairpin-like three-dimensional structure, which is known as the PP-fold [24]. However, they differ in their main location as NPY is primarily synthesized and released by neurons, PP is mainly found in endocrine pancreas and PYY is expressed in both neurons and gut endocrine cells. PYY is essentially produced in gut endocrine cells and released postprandially, a process which inhibits pancreatic secretion and gut motility [25,26]. PYY also reduces appetite [27]. Similarly, PP reduces pancreatic secretion, gut motility and appetite as well [28,29]. NPY is widely distributed in the central nervous system (CNS) as it is present in the basal ganglia, limbic system, amygdala, hippocampus, hypothalamus, septal nuclei and nucleus accumbens [30,31]. NPY is also detected in the peripheral nervous system, namely in the sympathetic nervous system, where it is co-localized with norepinephrine, and in a subpopulation of parasympathetic neurons [32].

NPY's physiological processes are mediated through the activation of different subtypes of NPY receptors belonging to the G-protein coupled receptors (GPCR) super family. The NPY receptors act via pertussis toxin-sensitive G-proteins, i.e., members of the G_i and G_o family, leading to the inhibition of adenylyl cyclase and, consequently, the decrease of cAMP accumulation in tissues and cells [33]. To date, six subtypes of NPY receptors have been described: Y_1 , Y_2 , Y_3 , Y_4 , Y_5 and y_6 . Until now, five of these have been cloned; with the exception of the Y_3 receptor, which has not been cloned and no specific agonist or antagonist have been attributed to it [34]. Comparisons between their sequences demonstrate that Y_1 , Y_4 and y_6 are more similar to each other than they are to the receptors Y_2 and Y_5 . Concerning the y_6 receptor, it has been cloned though its function is undetermined because it encodes for a truncated non-functional receptor in humans [33].

The Y_1 receptor was the first NPY receptor to be cloned. It embodies 384 amino acids and is typically expressed in postsynaptic sites. Its main agonists are NPY and PYY, even though it can also be activated by PP with a minor level of potency (Table 2). Highly selective agonists and antagonists with high binding affinities to the receptor subtype have been developed, shedding light on its physiological effects. Regarding Y_1 antagonists, the first non-peptide antagonist, which was highly potent and selective, that was discovered was (*R*)- N^2 -(diphenylacetyl)-*N*-[(4-hydroxyphenyl)methyl]-argininamide, commonly known as BIBP3226, that displays its affinity in the nanomolar range [35]. The high selectivity and specific binding to the Y_1 receptor has been demonstrated in numerous binding assays and in vitro and in vivo bioassays, with BIBP3226 being the most characterized Y_1 receptor antagonist.

The Y_2 receptor is a 381 amino acid protein with high affinities to NPY and PYY (Table 2). The particularity of this receptor lies in its presynaptic localization, leading to an autoreceptor role as it is involved in the inhibition of the release of NPY and other neurotransmitters [36]. In comparison to the Y_1 receptor, lower densities of expression of this receptor are observed in the mammalian brain [37].

The Y_4 receptor, a 375 amino acid peptide, is the only member of the NPY receptor family which has great affinity with PP as a ligand. PYY and NPY can also activate the receptor but they do so at a lower level of affinity (Table 2). The development of a peptide Y_4 agonist, BVD-74D, showed that it exhibited picomolar affinity for the receptor and it suppressed the food and water intake and weight gain of normal mice that were fed with normal diets and the food intake of normal mice that were fed with high-fat diets [38,39].

Concerning the Y_5 receptor, it has two isoforms that are pharmacologically alike: one long one that embodies 455 amino acids and one short one that is a splice variant that lacks the first 10 amino acids [40]. Both of these isoforms bind efficiently to NPY and PYY and have a lower affinity with PP (Table 2). The Y_5 receptor is strongly correlated with food intake, having been named initially as the "feeding receptor". Besides its localization

being in several areas of the brain—mainly the ones that regulate food intake, such as the hypothalamus—it was reported that NPY stimulated feeding via the Y_5 receptor [41]. Eröndu et al. reported their results concerning preclinical and clinical studies with the aim of testing the hypothesis that the antagonism of the Y_5 receptor leads to weight loss in overweight and obese patients [42]. The antagonist that was used in these studies was MK-0557 [43], a potent, highly selective, orally active Y_5 antagonist and the PET ligand was [^{11}C]MK0233, which has been used for receptor occupancy studies in rhesus monkeys and human volunteers. Interestingly, the authors concluded that Y_5 receptor antagonism did not induce clinically meaningful weight loss in obese patients.

Table 2. Characterization of NPY receptor subtypes.

Receptors	Endogenous Agonists in Order of Potency	Selective Agonists	Selective Antagonists	Expression	Functions
Y_1	NPY (0.2 nM) \geq PYY (0.7 nM) \gg PP (>100 nM) [33]	[Leu 31 ,Pro 34]NPY [44]; [Pro 34]NPY[Leu 31 ,Pro 34]PYY [45]; [Pro 34]PYY; [Phe 7 ,Pro 34]NPY [46]	BIBP3226 [35]; BIBO3304 [47]; SR120819A [48]; LY357897 [49]; J-115814 [50]; GI264879A [51]; GW1229 [52]; H394/84 [53]; PD160170 [54]; BMS-193885 [55]; BMS-205749 [56]; J-104870 [57]; BW1911U90[58]; T-190 [59]; T-241 [60]	Cerebral cortex, hippocampus, thalamus, hypothalamus, vascular smooth muscle cells, adipose tissue, kidney and gastrointestinal tract [61]	Feeding behavior [62,63]; inhibition of nociception [64]; regulation of hormone secretion [65]; ethanol consumption [66–68]; emotional behavior [69] and stress response [70]
Y_2	NPY (0.7 nM) \approx PYY (0.7 nM) \gg PP (>1000 nM) [33]	NPY $_{3-36}$; NPY $_{13-36}$; PYY $_{3-36}$, PYY $_{13-36}$ [45]; TASP-V [71]; Ac-[Lys 28 , Glu 32]- (25–36)-NPY [72]	T $_1$ [NPY $_{33-36}$] $_4$ [73]; BIIE0246 [74]; JNJ-5207787 [75]; JNJ-31020028 [76]; SF-11, SF-21, SF-22; SF-31, SF-41 [77]; ML072-ML075 [78]; CYM 948 and CYM 9552 [79]; 36 (GSK) [80]; 2 (GSK) [81]; [^3H]UR-PLN196 [82]	Hippocampus, hypothalamus, thalamus, amygdala, brainstem, spleen, liver, blood vessels, gastrointestinal tract and fat tissue [83–85]	Feeding behavior, anxiety, neuronal excitability and epilepsy and angiogenesis [86]; circadian rhythm [87]; alcohol dependence [88]; cognitive processes [89] and locomotor activity [90]
Y_3	NPY \geq NPY $_{13-36}$ \gg PYY, PP [18]	—	—	Hippocampus [91]; brain stem [92]; human adrenal medulla, rat superior cervical ganglia sympathetic neurons, rat <i>nucleus tractus solitarius</i> , rat cardiac ventricular membranes and rat distal colon [34,93]	Mediation of the NPY-induced secretion of catecholamines [93]
Y_4	PP (0.05 nM) $>$ NPY \approx PYY [33]	PP; GW1229 [94]; BW1911U90, T-190, T-241 [95]; BVD-74D [38];	UR-AK49 [96]	Hypothalamus, cerebral cortex, colon, small intestine, prostate, pancreas, skeletal muscle, thyroid gland, heart, stomach, adrenal medulla and nasal mucosa [97]	Food intake regulation [98]; luteinizing hormone release [99] and neuroprotection [100]
Y_5	NPY (0.6 nM) \geq PYY (1 nM) \geq PP [33]	D-[Trp 32]NPY [41]; D-[Trp 34]NPY [101]; [Ala 31 ,Aib 32]NPY [102]; [cPP $^{1-7}$, NPY $^{19-23}$, Ala 31 , Aib 32 ,Gln 34]-hPP [103]; [^{125}I]hPP $^{1-17}$,Ala 31 , Aib 32]NPY [104]; [^{125}I]cPP $^{1-7}$, NPY $^{19-23}$, Ala 31 , Aib 32 ,Gln 34]-hPP [105]; BWX-46 [106]	CGP71683A [107]; L-152,804 [108]; FMS-586 [109]; Lu AA33810 [110]; S 25585 [111]; NPY5RA-972 [112]; FR240662, FR252384 [113]; GW438014A [114]; NTNCB [115]; S-2367 (Velneperit) [116]; [^{11}C]MK-0233 [42]; MK-0557 [43]; [^{35}S]SCH 500946 [117]	Hypothalamus, cerebral cortex, amygdala, hippocampus and <i>Substantia nigra</i> [118] and intestine, ovary, testis, prostate, spleen, pancreas, kidney, skeletal muscle, liver, placenta and heart [97]	Appetite regulation, anxiolytic and anticonvulsant, regulation of circadian rhythms and inhibition of LH release [97]
Y_6	NPY \approx PYY $>$ PP [33]	—	—	Hippocampus, hypothalamus, heart and skeletal muscle [119,120]	Promotion of lean and bone mass acquisition in mice [121]

4. Development of PET Tracers for NPY Receptors

As PET imaging is a powerful tool for drug development, especially when the target is in the central nervous system, the ability to develop successful radiotracers becomes significant as well. Radiotracers can have different roles in the drug development process: they can be used to demonstrate target delivery, to observe the change in the biochemistry of a system and to show the occupancy of a targeted site. In order to obtain an excellent radiotracer, some requirements must be fulfilled. Firstly, the radiotracer needs to have a high level of affinity towards the target, which requires the prior identification of the target of interest and then the development of ligands with high affinity to the target. Ideally, it is stipulated that the ratio $B_{\text{max}}/K_d > 10$ (as B_{max} represents the target site concentration and K_d the equilibrium dissociation constant of the radiotracer for that site) is met in order to have a high probability of the detection of the specific binding in vivo (even

though there are some exceptions). Lipophilicity, expressed as Log P, is of relevance as it can influence the extent of the nonspecific binding activity and the ability to cross lipid membranes. Log P should be between 1 and 3.5 (though it is preferable that it is less than 3) for appropriate brain penetration and a good specific–non-specific binding ratio. In addition, the radiotracer must not be a P-glycoprotein (P-gp) substrate, as this is an efflux transporter that is substantially expressed in blood–brain barrier (BBB) penetration, blocking brain penetration. Ultimately, the radioligand should have an easy radiolabeling precursor, which means that the ligand should have chemical structural features that are suitable for radiolabeling with the appropriate radionuclide. The main goal in this step is to utilize a radiotracer with high molar activity, high radiochemical purity and high radiochemical yield. For further information about the main aspects of in vivo site-directed radiotracers, see Patel et al. [122].

4.1. NPY Y₁ Receptor

Over the past years, Y₁ receptor antagonists have been developed in order to study the diverse physiological roles of their receptors. In order to further understand the physiological role of Y₁ receptors in vivo, the development of novel PET tracers that are suitable for Y₁ receptors would allow the non-invasive imaging of the same and the determination of their occupancy. Bearing this in mind, Kameda et al. synthesized a series of 2,4-diaminopyridines and evaluated their suitability to become a PET tracer for the Y₁ receptor [123]. This investigation started with the identification of lead compound **1** (Figure 1) as a promising PET tracer during structure-activity relationship studies. Compound **1** showed appropriate lipophilicity (Log P = 3.0) and favorable characteristics to be radiolabeled with ¹⁸F; however, it was shown to have only a moderate level of Y₁ receptor binding affinity (Y₁ IC₅₀ = 21 nM). Thus, the focus of the study was on improving the affinity of the lead compound **1** towards the Y₁ receptor and its lipophilicity.

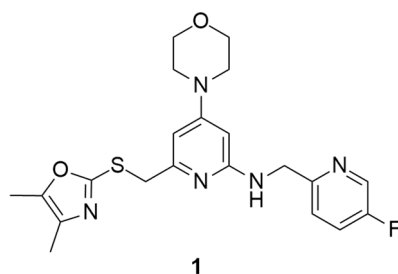


Figure 1. Structure of Y₁ receptor antagonist **1**.

The SAR studies led to the identification of the potent and selective compounds **1d** and **1e** (Tables 3 and 4) as promising candidates for Y₁ PET tracers. Firstly, the variation of the antagonist **1** right hand 2-amino group was examined and the 2-fluoro-6-methylenepyridine derivative showed the most potent Y₁ affinity (Y₁ IC₅₀ = 1.5 nM, compound **1a**, Table 3). Bearing this result, this derivative was substituted with other proper functional groups in order to favor its use in radiolabeling. The replacement of the fluorine with a methyl group resulted in a powerful increase in the level of binding affinity (Y₁ IC₅₀ = 0.69 nM, compound **1b**, Table 3) and a subtle reduction of the lipophilicity. Then, the left hand heterocycle portion of the previous compound was optimized. The 4,5-dimethyloxazole ring was replaced with a 4,5-dimethylthiazole ring, an atom of fluorine was attached to the 5-methyl group (compound **1c**, Table 3) and, lastly, the fluorine was moved from the 5-methyl to a 4-methyl group of the thiazole ring so as to produce compound **1d** with its high affinity towards the Y₁ receptor and reduced lipophilicity (Table 3). Notably, this fluorine substitution is an additional labelling option for the incorporation of ¹⁸F via nucleophilic substitution. Moreover, the 4-fluoromethyl-5-ethyl-thiazole derivative (compound **1e**) showed an even further improvement in Y₁ receptor binding and reasonable lipophilicity

(Table 3). Both compounds **1d** and **1e** also exhibited great selectivity towards the Y₁ receptor (Table 4).

Table 3. SAR of compounds **1a–e**.

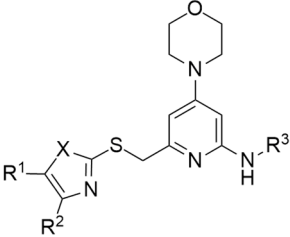
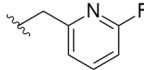
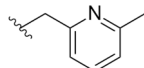
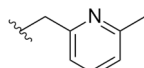
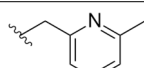
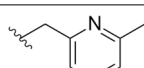
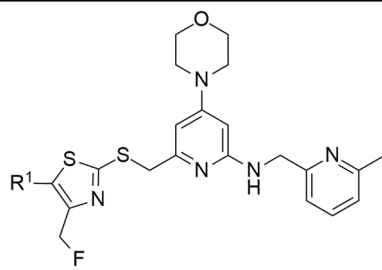
						
Compound	X	R ¹	R ²	R ³	Y ₁ Binding Affinity IC ₅₀ (nM)	Log P
1a	O	CH ₃	CH ₃		1.5	3.1
1b	O	CH ₃	CH ₃		0.69	2.8
1c	S	CH ₂ F	CH ₃		0.56	2.3
1d	S	CH ₃	CH ₂ F		0.20	2.7
1e	S	CH ₂ CH ₃	CH ₂ F		0.13	3.2

Table 4. Structure and in vitro properties of compound **1d** and **1e** (Y1-973).

					
Compound	R ¹	Y ₁ IC ₅₀ (nM)	Y ₂ , Y ₄ , Y ₅ IC ₅₀ (μM)	Log P	P-gp Transport Ratio
1d [123]	CH ₃	0.20	>10	2.7	1.8
1e (Y1-973) [123,124]	CH ₂ CH ₃	0.13	>10	3.2	1.4

Afterwards, Hostetler et al. identified Y₁-973 (compound **1e**) as a promising PET tracer candidate to be radiolabeled as it fulfilled the abovementioned requirements: potency < 0.5 nM, Log P < 3.5, P-gp ratio < 3 and it was suitable for radiolabeling with ¹⁸F. Thus, the authors were able to report the synthesis and pre-clinical evaluation of the NPY Y₁ receptor PET tracer [¹⁸F]Y₁-973 [124]. [¹⁸F]Y₁-973 was produced through the reaction of [¹⁸F]KF/K₂₂₂ with the t-butyloxycarbonyl (Boc)-protected chloromethyl thiazole **2** precursor in DMSO at 130 °C using microwave heating, followed by deprotection with 1 M HCl (Figure 2). [¹⁸F]Y₁-973 was obtained in satisfactory radiochemical yields (18 ± 13%, *n* = 9) with >98% radiochemical purity and high molar activity (1548 ± 859 Ci/mmol), in a total synthesis time, including purification by semi-preparative HPLC, of about 45 min [124].

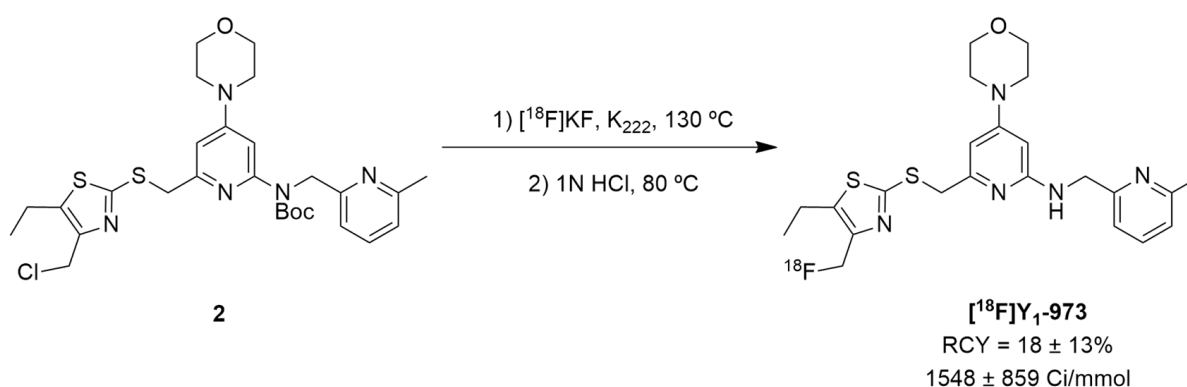


Figure 2. The radiosynthesis of the NPY Y₁ PET tracer [¹⁸F]Y₁-973.

In vivo PET imaging studies of [¹⁸F]Y₁-973 in rhesus monkeys have demonstrated that this PET tracer promptly penetrates the blood–brain barrier. Baseline PET scans of this radiotracer in rhesus monkeys have shown heterogeneous distribution throughout the brain, with a pattern of uptake that is consistent with the known high NPY Y₁ brain density (the highest level of uptake was in the striatum and cortical regions, there was moderate uptake in the thalamus and low uptake in the cerebellum). [¹⁸F]Y₁-973 also exhibited rapid kinetics in rhesus monkeys' brains, with the uptake peaking in the striatum at approximately 30 min. Additionally, it has a large binding potential that is suitable for receptor occupancy PET studies with an NPY Y₁ antagonist [124].

Hofmann et al. reported a suitable ¹⁸F-labeled high-molecular weight glycopeptide for the imaging of peripheral NPY Y₁ receptor-positive tumors, namely breast cancer. Notably, the human Y₁ receptor subtype has been discovered to be overexpressed in 85% of primary breast cancer and in 100% of lymph node metastases [125]. Despite [¹⁸F]Y₁-973 having remarkable properties for brain imaging of the Y₁ receptor, its high lipophilicity and significant liver accumulation makes it less suitable for peripheral application for breast cancer imaging. Therefore, the authors reported the development of a full length NPY analogue bearing a glycosylation site in position 4 of the amino acid sequence and the ¹⁸F-labeling by ¹⁸F-fluoroglycosylation using click chemistry (Figure 3) [126].

The authors selected [F⁷, P³⁴] NPY analogue as it had scientific evidence supporting its selective binding to Y₁ receptor and they then developed two peptide precursors bearing an alkyne-bearing functionality (peptides **5a** and **6a**, Figure 3), allowing regiospecific ¹⁸F-labeling by ¹⁸F-fluoroglycosylation using click chemistry. The alkyne functionalization was obtained by the introduction of propargylglycine (Pra) at position 4 (Figure 3).

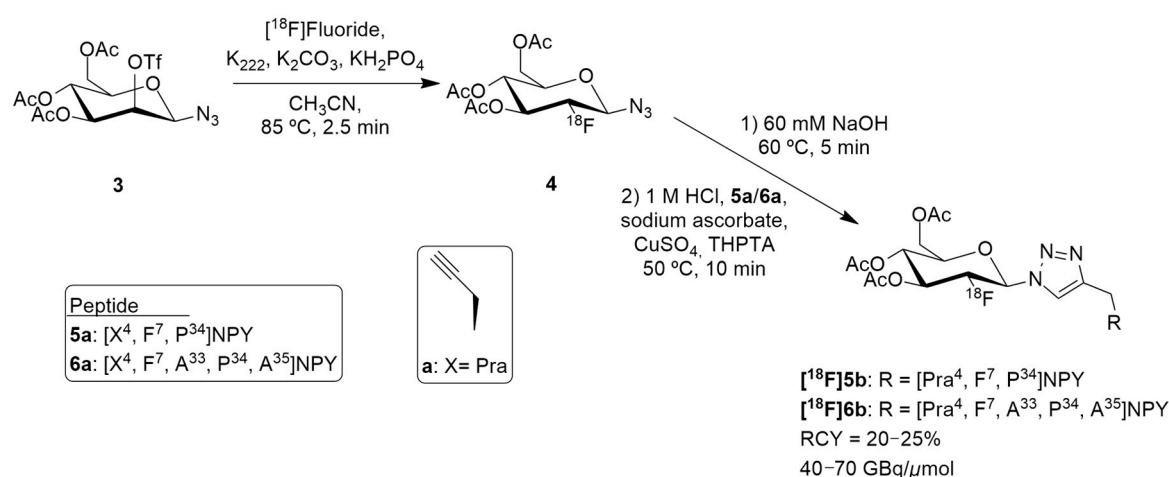


Figure 3. Radiosynthesis of [¹⁸F]5b and [¹⁸F]6b.

¹⁸F-Fluoroglycosylated NPY analogues [¹⁸F]5b and [¹⁸F]6b were obtained through the course of different reactions (Figure 3). Firstly, the precursor 3,4,6-tri-O-acetyl-2-O-trifluoromethanesulfonyl-β-D-mannopyranosyl azide 3 reacted with [¹⁸F]fluoride, K₂₂₂ and potassium carbonate in acetonitrile, resulting in the formation of 2-deoxy-2-[¹⁸F]fluorogluco pyranosyl azide 4. Then, the remaining solution (60 mM NaOH) was adjusted to pH 8 (1M HCl) and a solution of the peptides 5a or 6a, sodium ascorbate, CuSO₄ and THPTA (tris(hydroxypropyltriazolylmethyl)amine) were added. After isolation by semipreparative HPLC and subsequent solid phase extraction, [¹⁸F]5b (*n* = 7) or [¹⁸F]6b (*n* = 2) were obtained. The molar activities were about 40–70 GBq/μmol in overall radiochemical yields of 20–25% with a total synthesis time of 75 min. Further in vitro characterization was undertaken and the glycopeptide [¹⁸F]5b showed great selectivity for Y₁ receptor over the Y₂ receptor and strong Y₁ receptor internalization. In this study, the preclinical animal model that was used was an MCF-7 breast cancer tumor model. PET imaging studies in these animals demonstrated a specific binding uptake of the glycopeptide [¹⁸F]5b from Y₁ receptors present in MCF-7 tumors and that [¹⁸F]5b exhibited considerably increased renal clearance properties, compared to the NPY DOTA-derivatives, showing favorable kinetics in vivo [126].

As mentioned earlier, 85% of mammary carcinomas are Y₁ receptor positive. To address this issue, Keller et al. reported the exploration of ¹⁸F-labeled compounds that were derived from the argininamide BIBP3326, which is a Y₁ receptor antagonist (Figure 4) [127].

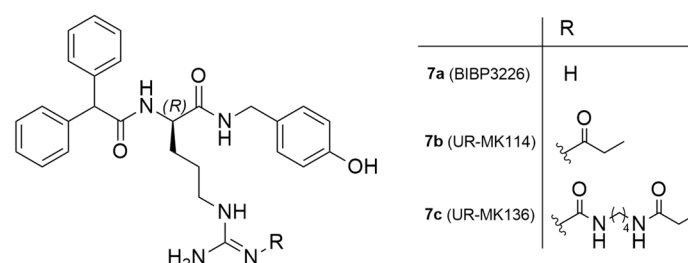


Figure 4. Chemical structure of Y₁ receptor antagonist BIBP3326 and Y₁ ligands derived from argininamide-type antagonists.

The authors acknowledged that the bioisosteric substitution of the guanidine group in the argininamide moiety of a BIBP3326 compound (e.g., UR-MK114, 7b and UR-MK136, 7c, Figure 4) was shown to lead to the formation of highly selective and potent fluorescent ligands, bivalent ligands and tritiated radioligands for the Y₁ receptor. Similarly, Keller et al. used this strategy to design new and selective [¹⁸F] Y₁ receptor PET ligands. After the synthesis and in vitro characterization of a series of fluorinated argininamides, they

concluded that derivative **10** (Figure 5) was the most promising candidate as it displayed the lowest lipophilicity (Log P of 3.4). Derivative **10** was synthesized using the building block **8**. The radiosynthesis of [^{18}F]**10** was proceeded by the treatment of excess of amine **9** with [^{18}F]**8** (Figure 5). [^{18}F]**8** was, beforehand, obtained by the ^{18}F -fluorination of the 9'-anthrylmethyl-2-bromopropionate precursor, under mild conditions and in the presence of KH_2PO_4 , followed by isolation by semipreparative HPLC. [^{18}F]**10** was obtained in an overall RCY of 5–8% (uncorrected for decay) in an overall synthesis time of 70–80 min, with a radiochemical purity of >99% and a molar radioactivity of 12–21 GBq/ μmol ($n = 6$) [127].

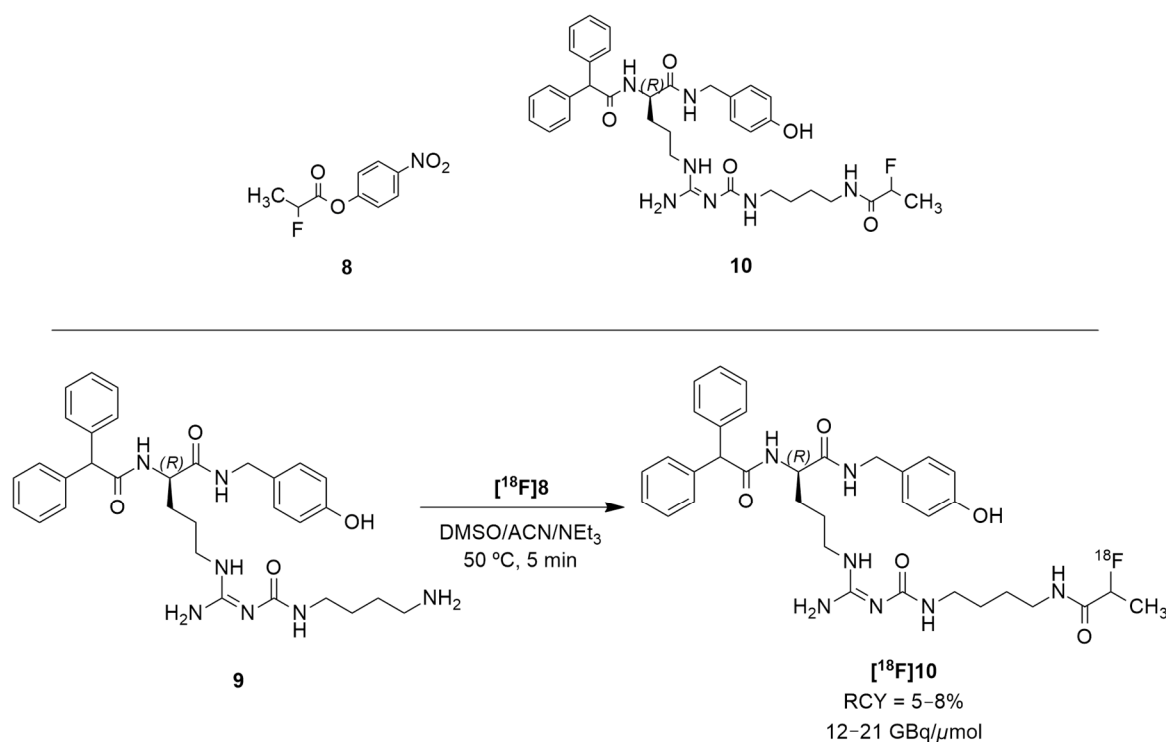


Figure 5. Radiosynthesis of [^{18}F]**10**.

The tracer [^{18}F]**10** was then evaluated *in vitro* and *in vivo* using tumor-bearing nude mice with Y_1R positive MCF-7 tumors. Its Log P was experimentally determined resulting in a value of 2.34 ± 0.03 . [^{18}F]**10** had fast blood clearance time at 30 and 90 min, low uptake in the liver and high uptake in the gallbladder and intestines. The tracer also showed high tumor retention and a suitable signal-to-noise ratio for PET imaging. In comparison with [^{18}F]**5b**, [^{18}F]**10** had lower tumor uptake because of its uptake in the gallbladder. Nonetheless, [^{18}F]**10** showed diminished kidney uptake when compared with the peptide tracer, which is the major advantage of the nonpeptide radioligand over the peptide tracer for PET imaging. *In vivo* PET imaging studies with the antagonist [^{18}F]**10** in the MCF-7 nude mice revealed the visualization of Y_1R -positive MCF-7 tumors [127].

Regarding these results and in order to reduce the lipophilicity of a candidate ligand and to achieve more suitable biodistribution with minimal biliary excretion, hence improving the tumor visibility in PET images, Maschauer et al. recently reported the synthesis and radiosynthesis of three BIBP3226 derivatives that were conjugated with ^{18}F -fluoroethoxy linkers and ^{18}F -fluoroglucosyl moiety and further *in vitro* and *in vivo* characterization [128]. [^{18}F]**15** was obtained through a copper-catalyzed azide–alkyne cycloaddition (CuAAC-Based) ^{18}F -fluoroglycosylation method between the BIBP3226 derived alkyne **11** and 6-deoxy-6-[^{18}F]fluoroglucosyl azide [^{18}F]**12** (Figure 6). [^{18}F]**12** was previously prepared and isolated by semi-preparative HPLC and deacetylated with NaOH, following a previously described method [129]. [^{18}F]**15** was then isolated by semi-preparative radio-HPLC, with a radioactivity yield (RAY) of about 20% (in reference to [^{18}F]fluoride),

molar activity of 9 GBq/ μmol and radiochemical purity >99% in a total synthesis time of 80 min. [^{18}F]16 and [^{18}F]17 were attained using the same protocol as [^{18}F]15, apart from the deprotection step. [^{18}F]13 and [^{18}F]14 were provided by the [^{18}F]-labelling of their corresponding tosylate-bearing precursors, with radioactivity yields of 38% and 40%, in total synthesis times of 40 min and 35 min, respectively. Afterwards, they were treated with the BIBP3226-derived alkyne **11** in a click chemistry reaction under similar conditions as those which were used for the glucosyl derivative [^{18}F]15. [^{18}F]16 and [^{18}F]17 were isolated with radioactivity yields of about 5% and 10% (in reference to [^{18}F]fluoride), molar activities between 5–6 GBq/ μmol and radiochemical purity >99% in a 60 min total synthesis time (Figure 6).

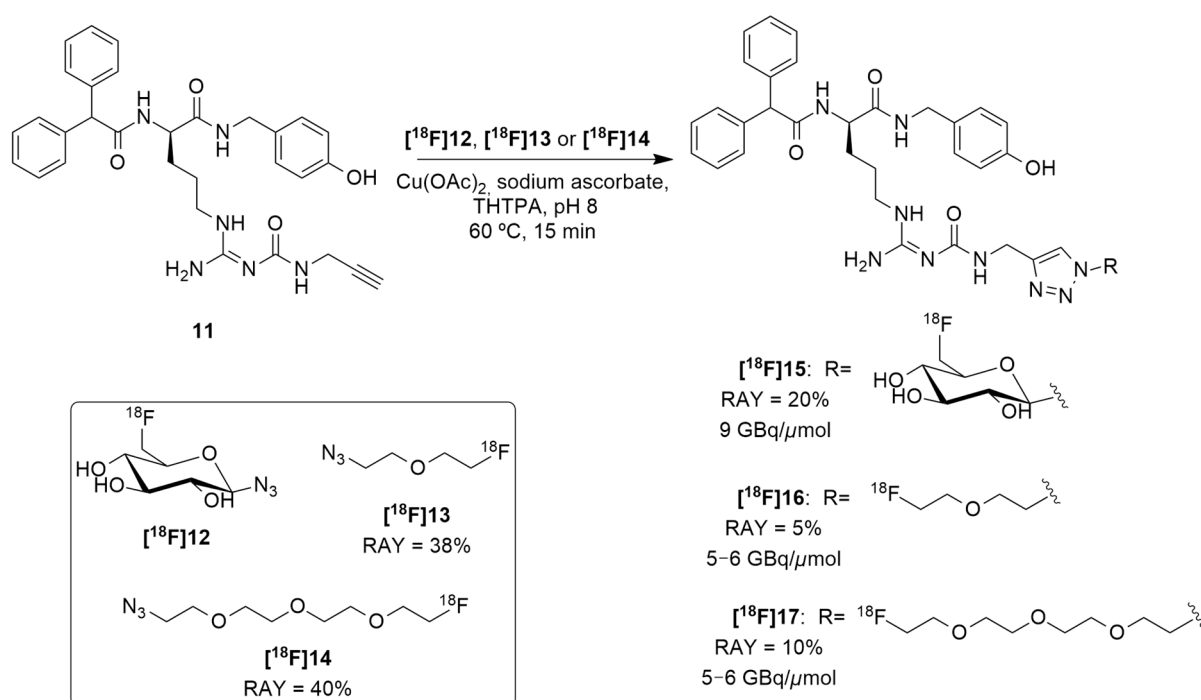


Figure 6. Radiosynthesis of [^{18}F]15, [^{18}F]16 and [^{18}F]17.

The *in vitro* characterization of the three compounds showed that these were selective towards the Y_1 receptor and revealed their weak lipophilicity, with [^{18}F]15 being the most hydrophilic compound and [^{18}F]16 being the least hydrophilic one ([^{18}F]15 Log P = 0.78, calculated: 0.43; [^{18}F]17 Log P = 1.49, calculated: 1.94; [^{18}F]16 Log P = 1.74, calculated: 2.03). This characterization also showed the stability of all three of the radioligands as no radioactive degradation products were shown with 3 h of incubation. Regarding the cellular accumulation, the human breast cancer cells MCF-7- Y_1 were used, wherein it was noticed that there was the highest specific accumulation of [^{18}F]16, mainly explained by the high affinity of this ligand. The other two showed low or non-specific binding to MCF-7- Y_1 cells. In autoradiography experiments, [^{18}F]16 and [^{18}F]17 have demonstrated marked specific binding to the solid MCF-7- Y_1 tumors, whereas [^{18}F]15 showed very low specific binding. Biodistribution studies have indicated that, generally, all three of these radioligands are similar to [^{18}F]10 as moderate amounts of radioactivity were detected in the kidneys and intestines and extraordinarily high radioactivity was observed in the gallbladder. Thus, the aim of achieving a reduced level of uptake in the gallbladder by using more hydrophilic compounds was not reached, although it was possible to reduce the lipophilicity of the analogues. Blood sample analysis by HPLC revealed that the radiotracers [^{18}F]16 and [^{18}F]17 underwent rapid degradation, resulting in the formation of hydrophilic radiometabolites, while [^{18}F]15 was more stable in the blood *in vivo*. Finally, PET imaging was performed and the radiotracer [^{18}F]15 did not allow the visualization

of the tumor, most likely due to its poor affinity to the receptor. Both radioligands [^{18}F]**16** and [^{18}F]**17** showed specific tumor accumulation *in vivo*, even though there were relatively high background values in the PET images, due to the formation of radiometabolites in the blood.

Recently, the radiolabeling of the Y_1 antagonist BMS-193885 with [^{11}C] has also been reported [130]. BMS-193885 (1,4-dihydro-3-[[[3-[4-(3-methoxyphenyl)-1-piperidinyl]propyl]amino]carbonyl]amino]phenyl]-2,6-dimethyl-3,5-pyridinedicarboxylic acid, dimethyl ester, **18**, Figure 7) is a potent and selective NPY Y_1 receptor antagonist with good brain penetration and systemic bioavailability but poor oral bioavailability [55,131]. It was previously disclosed that it reduces food intake and body weight in animal models of obesity, being pharmacologically efficacious in the treatment of obesity in animal models [131]. Therefore, Kawamura et al. reported the radiolabeling of **18** in two different ways: the first one involved the methylation of the desmethyl analog **19** (via A, Figure 8) with [^{11}C]methyl iodide and the other one involved the radiosynthesis of [^{11}C]desmethyl BMS-193885 ([^{11}C]**22**, via B, Figure 8), using [^{11}C]phosgene as the radiolabeling agent [130].

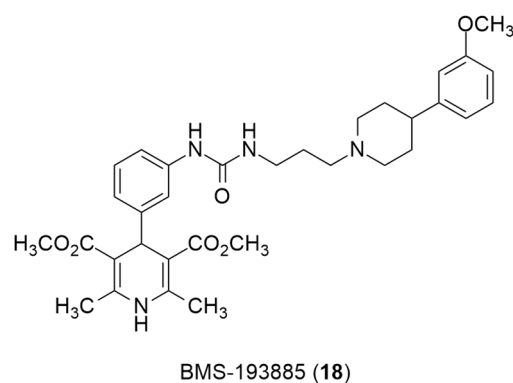


Figure 7. Chemical structure of Y_1 receptor antagonist BMS-193885(**18**).

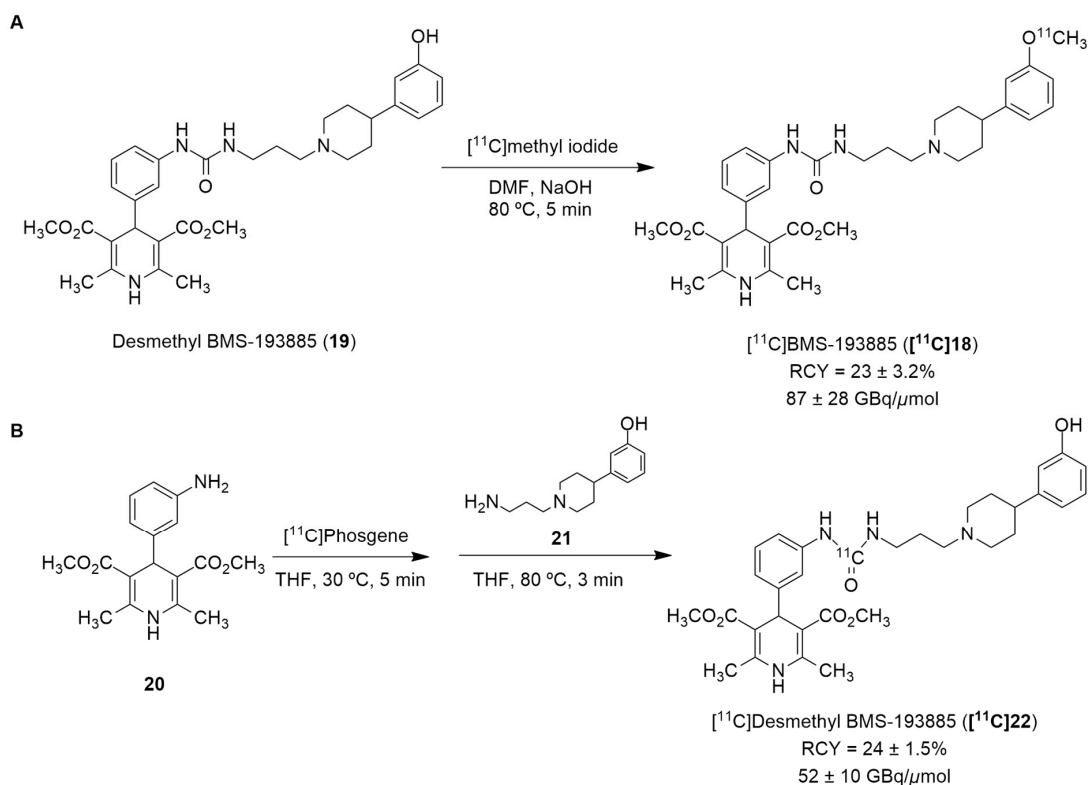


Figure 8. Radiosynthesis of [^{11}C]**19** via [^{11}C] CH_3I (A) and [^{11}C]**22** via [^{11}C]phosgene (B).

In order to obtain the tracer [^{11}C]**18**, an automated synthesis system that was developed in-house was used. A solution of **19** and sodium hydroxide solution in *N,N*-dimethylformamide (DMF) was added to a dry septum-equipped vial prior to the reaction. [^{11}C]Methyl iodide was produced by the reduction of cyclotron-produced [^{11}C]carbon dioxide with lithium aluminum hydride, followed by iodination with hydroiodic acid. The [^{11}C]methyl iodide that was produced was then trapped in a reaction vial containing **19** in DMF. The reaction mixture was heated and held at 80 °C for 5 min. Afterwards, the solution was purified by preparative HPLC. [^{11}C]**18** was synthesized approximately 30 min after the end of irradiation (EOI), with a radiochemical yield of $23 \pm 3.2\%$ ($n = 6$), molar activity of 87 ± 28 GBq/ μmol ($n = 6$) and radiochemical purity >99% (Figure 8A). The radiosynthesis of [^{11}C]**22** (Figure 8B) started with the initial production of [^{11}C]carbon dioxide using a cyclotron, followed by the subsequent reduction of [^{11}C]carbon dioxide with H_2 in the presence catalyst, generating [^{11}C]methane, the chlorination of [^{11}C]methane and the conversion of [^{11}C]carbon tetrachloride to [^{11}C]phosgene. Afterwards, aniline derivative **20** in a tetrahydrofuran (THF) solution was added to a dry septum-equipped vial just prior to radiosynthesis. [^{11}C]phosgene was trapped in the solution containing **20** at -15 °C for 1 min. The reaction mixture was heated at 30 °C for 3 min. When the solution cooled, it was added a solution containing amine derivative **21** in THF. Then, the reaction mixture was heated at 80 °C for 3 min in order to remove the THF. The crude product was then purified through the use of preparative HPLC. Finally, [^{11}C]**22** was obtained at about 33 min after EOI with a radiochemical yield of $24 \pm 1.5\%$ ($n = 4$), molar activity of 52 ± 10 GBq/ μmol ($n = 4$) and radiochemical purity >99% (Figure 8B) [130].

In vivo studies have shown poor brain penetration from both of these radiotracers. The synthesis of [^{11}C]**22** was undertaken mainly in order to address the issue of the poor brain penetration of [^{11}C]**18**, as it has lower lipophilicity (Log P = 3.3) than [^{11}C]**18** (Log P = 3.8) and higher affinity binding ([^{11}C]**22** $K_i = 2.7$ nM and [^{11}C]**18** $K_i = 3.3$ nM). Nevertheless, the radioactivity in the brain of [^{11}C]**22** was much lower than that of [^{11}C]**18**, mostly due to its faster metabolization (high levels of [^{11}C]**22** were present in the small intestine and liver). The poor brain penetration of [^{11}C]**18** is mainly explained by the influence of the drug efflux transporters P-gp and BCPR. Therefore, in order to visualize the NPY Y_1 receptors in the brain using this strategy, it is crucial to develop PET tracers with superior blood–brain barrier penetration and in vivo stability. Nevertheless, this study was useful in its provision of a better understanding of the in vivo properties of **18**.

Diverging from the classical methods of the radiolabeling of the Y_1 antagonists, Vall-Sagarra et al. combined the use of heterobivalent peptidic ligands (HBPLs) with [^{68}Ga] radiolabeling methods and developed a distinct approach to the development of new Y_1 radiotracers [132]. As is known, radiolabeled peptides are a great tool for tumor visualizations as they target the many receptors that are overexpressed, though normally they target a specific receptor. As different tumor lesions can express different receptor types, the tumor visualization may not be as efficacious as it was previously hypothesized. Radiolabeled heterobivalent peptide ligands (HBPLs) have the capacity to specifically target more than one receptor type, rendering them advantageous when compared to monovalent peptides, enabling better tumor visualization and improved in vivo biodistribution. As was referenced earlier, human breast cancer overexpresses 85% of NPY Y_1 receptor but, as a matter of fact, it also overexpresses the gastrin-releasing peptide receptor (GRPR) in about 75% of cases. Hence, the authors developed bispecific HBPLs and radiolabeled them with ^{68}Ga and then proceeded to undertake further in vitro and in vivo characterizations in order to show the general feasibility of this distinct strategy. Thus, HBPLs **23–27** and monomeric reference peptides **28** and **29** (Figure 9) were synthesized and then radiolabeled with Ga^{3+} . The $^{68}\text{Ga}^{3+}$ was obtained via the elution of an $^{68}\text{Ge}/^{68}\text{Ga}$ generator system. Then, the pH of the solution was adjusted from 3.5 to 4.0 and the NODA-GA-comprising HBPLs **23–27** was incubated at 40–45 °C for 10 min. The DOTA-comprising reference compounds **28** and **29** reacted at 99 °C under identical conditions. The radiolabeled products [^{68}Ga]**23**–[^{68}Ga]**27**, [^{68}Ga]**28** and [^{68}Ga]**29** were attained in radiochemical yields and purities of 95–99% with

After the analysis of the *in vitro* studies' results, the authors selected HBPL [⁶⁸Ga]25 to be used in the *in vivo* evaluations as, compared to the other HBPLs that were developed, it showed the highest stability and hydrophilicity as well as a slightly greater level of tumor cell uptake. Thus, small animal PET/CT imaging studies in T-47D tumor-bearing immunodeficient mice were performed using the HBPL [⁶⁸Ga]25 and also the scrambled variants: [⁶⁸Ga]25a (PESIN_{scrambled} combined with [Lys⁴(aminoxy), Trp⁵, Nle⁷]BVD₁₅) and [⁶⁸Ga]25b (PESIN combined with [Lys⁴(aminoxy), Trp⁵ and Nle⁷]BVD_{15,scrambled}), under identical conditions. The *in vivo* PET/CT imaging and *ex vivo* biodistribution data showed high kidney and liver uptakes. Regarding the tumor visualization, the scrambled analogs [⁶⁸Ga]25a and [⁶⁸Ga]25b were less efficient compared to the bispecific ligand [⁶⁸Ga]25, a finding that indicates that both parts of HBPL [⁶⁸Ga]25 were necessary to enhanced *in vivo* tumor uptake and that this uptake was GRPR- and NPY Y₁-specific. Concluding, the authors were able to demonstrate that the use of GRPR- and NPY Y₁-specific HBPL were indeed beneficial to *in vivo* tumor uptake and visualization, compared to monospecific agents [132].

Recently, Krieger et al. have reported the synthesis of ⁶⁸Ga-radiolabeled analogues of the most promising previously described truncated NPY analogues and compared them regarding their metabolic stability [133]. Of the nearly 80 truncated peptides analogues of NPY that have been developed over the years, the authors chose the following five by virtue of their metabolic stability: linear [Pro³⁰,Lys(DOTA)³¹,Tyr³²,Leu³⁴]NPY₂₈₋₃₆ ([Lys⁴(DOTA)]-BVD₁₅), **30**; [Pro³⁰,Lys(DOTA)³¹,Bip³²,Leu³⁴]NPY₂₈₋₃₆, **31** (Bip: biphenylalanine); [Lys(lauroyl)²⁷,Pro³⁰,Lys(DOTA)³¹,Bip³²,Leu³⁴]NPY₂₇₋₃₆, **32**; Ac[D-Cys²⁹,Lys(DOTA)³¹,Cys³⁴]NPY₂₉₋₃₆, **33** and heterodimer [Pro³⁰,Cys³¹,Trp³²,Nle³⁴]NPY₂₈₋₃₆-[Lys(DOTA)²⁹,Pro³⁰,Cys³¹,Trp³²,Nle³⁴]NPY₂₈₋₃₆, **34**. The monomers **30–33** and heterodimer **34** were radiolabeled with ⁶⁸Ga³⁺ (which was obtained by the fractionated elution of an IGG ⁶⁸Ge/⁶⁸Ga generator system) in an aqueous acetate-buffered solution. The radiolabeling reaction occurred at 99 °C, for a duration of 10 min at a pH level of 3.5–4.0. The products [⁶⁸Ga]30–[⁶⁸Ga]32 and [⁶⁸Ga]34 were obtained in high radiochemical yields and purities of 96–99% and with non-optimized molar activities of 18.8–23.1 GBq/μmol, starting from 376.6–461.0 MBq of ⁶⁸Ga³⁺. Pure [⁶⁸Ga]33 could not be obtained through these reaction conditions due to the formation of a significant number of side products. Despite the authors' efforts to find out the origin of those side products, the origins remained inconclusive and so further [⁶⁸Ga]33 characterization and stability evaluation was omitted. The Log P values were determined and they showed an increasing variation from the hydrophilic [⁶⁸Ga]30, with a Log P value of -3.61 ± 0.37 , to lipophilic [⁶⁸Ga]32, with a Log P value of -0.48 ± 0.14 and the heterodimer [⁶⁸Ga]34 showed a hydrophilic character as well, with a Log P value of -2.47 ± 0.18 . The stability of these four radioligands was determined by the use of a human serum and human microsomal stability assay. Regarding the human serum stability assay, the radioligands showed the formation of different hydrophilic metabolites and considerable differences concerning their rate of degradation by peptidases, which caused a great difference in the half-lives of the compounds. [⁶⁸Ga]30 showed a low stability in the serum with a half-life of 20 min. The modification of the Tyr³² amino acid by artificial Bip in [⁶⁸Ga]31 led to a higher half-life of this radioligand, which amounted to 65 min, ensuring higher stabilization against degradation. The additional N-terminal lauroylation in [⁶⁸Ga]32 further increased the serum stability of the radiotracer, resulting in a half-life of 144 min, one which is more than adequate for ⁶⁸Ga-PET imaging uses as PET scans using ⁶⁸Ga are usually performed within the first 60 to 90 min post injection. Comparable to [⁶⁸Ga]31, [⁶⁸Ga]34 showed a half-life of 67 min. Regarding the liver microsomal stability assay, the same stability trend was found within the radiopeptides [⁶⁸Ga]30–[⁶⁸Ga]32, with [⁶⁸Ga]32 being the most stable among them. Heterodimer [⁶⁸Ga]34 was degraded more rapidly by the liver enzymes than in the human serum assay, presenting a half-life of only 6 min. Thus, [⁶⁸Ga][Lys(lauroyl)²⁷,Pro³⁰,Lys(DOTA)³¹,Bip³²,Leu³⁴]NPY₂₇₋₃₆ ([⁶⁸Ga]32) was the most promising truncated NPY analogue for the development of peptide-based NPY Y₁ receptor imaging agents within this study. It showed excellent *in vitro* receptor binding

affinity and a very high level of stability towards proteolytic degradation by peptidases, both in human serum and in the human liver.

More recently, still focusing on *in vivo* receptor targeting with radiolabeled peptide-based probes, Cardoso et al. described the development and characterization of two ^{68}Ga -labeled NPY analogues for their potential use in breast cancer diagnosis [134]. Both of the analogues shared the same amino acid sequence: Tyr-Arg-Leu-Arg-BPA-Nle-Pro-Asn-Ile (BPA: L-4-benzoylphenylalanine), one which favors preferential binding to NPY Y_1 receptors, and were derivatized with NOTA (Figure 10) through a lysine (35a) or an acetylated lysine (35b) linker.

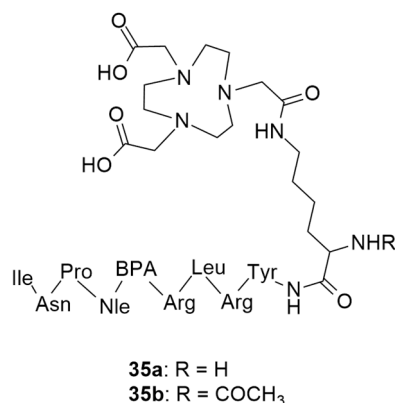


Figure 10. Structures of short NPY analogues functionalized with NOTA (35a and 35b).

The authors assessed different labelling reaction conditions, such as various peptide masses (50, 100 or 150 μg), incubation temperatures (20 and 95 $^{\circ}\text{C}$) and reaction times (5 and 10 min). The best radiolabeling conditions were found to be 100 μg of ligand, a pH of 4.5, 5 min incubation time and 95 $^{\circ}\text{C}$ incubation temperature. With these conditions, both radiopharmaceuticals [^{68}Ga]35a and [^{68}Ga]35b showed radiochemical purities that were higher than 95% and neither gallium colloids nor $^{68}\text{GaCl}_3$ were detected. Afterwards, the physicochemical properties were evaluated. Both of the complexes were hydrophilic, with Log P values of -3.2 ± 0.1 for [^{68}Ga]35a and -2.6 ± 0.1 for [^{68}Ga]35b, though the authors argue that these Log P values should not negatively affect the cellular uptake of the complexes as it depends on the expression of the NPY receptors on the cellular surface. In general, both of the complexes showed great *in vitro* stability, good cellular uptake, binding affinities in the nanomolar range and high cellular internalization rate. Interestingly, both of the complexes showed significant differences in their cellular uptake and externalization rates, as well as their Log P values. As the complex [^{68}Ga]35b has a modified lysine, this makes it less hydrophilic and, consequently, increases its cellular uptake and reduces its externalization rate. Regarding their biodistribution profiles, both of the radiolabeled compounds had a high rate of blood depuration and renal excretion, being consistent with their hydrophilicity. However, the tumor uptake was moderate and ratio of tumor-to-muscle and tumor-to-blood were not as high as those which have been reported in the literature as being the most promising for diagnostic imaging. Nonetheless, these studies have shed light on the influence of the labelling technique in the development of new promising radiopharmaceuticals.

4.2. NPY Y_2 Receptor

Winterdahl et al. reported the development of the first and, to date, the only PET radiotracer for the Y_2 receptor [135]. The authors took advantage of the suitable characteristics of the Y_2 receptor antagonist JNJ-31020028 (36, Figure 11) and radiolabeled this compound using [^{11}C]CH₃I in order to visualize the Y_2 receptors in the living brain. JNJ-31020028 (*N*-(4-(4-[2-(diethylamino)-2-oxo-1-phenylethyl]piperazin-1-yl)-3-fluorophenyl)-2-pyridin-3-ylbenzamide) is a Y_2 receptor antagonist with high affinity and selectivity for

the receptors, poor oral availability (6%) in rats but high bioavailability subcutaneously (100%) and a half-life of 0.83 h. It penetrates the blood–brain barrier and occupies 90% (at 10 mg/kg) of the Y_2 receptors [76]. The radiosynthesis of *N*-[^{11}C]-methyl-JNJ-31020028 ($[^{11}\text{C}]\mathbf{37}$) was performed in an semiautomated system wherein [^{11}C]methyl iodide was produced from [^{11}C]CO₂. [^{11}C]CH₃I was trapped in a solution of **36** and NaH dissolved in DMF and THF. The reaction occurred over the course of 3 min at 50 °C (Figure 11). The crude product was then purified by preparative HPLC and the radiolabeled compound [^{11}C]**37** was obtained with radiochemical purity > 98% and molar activity > 100 GBq/ μmol (the radiochemical yield was not disclosed).

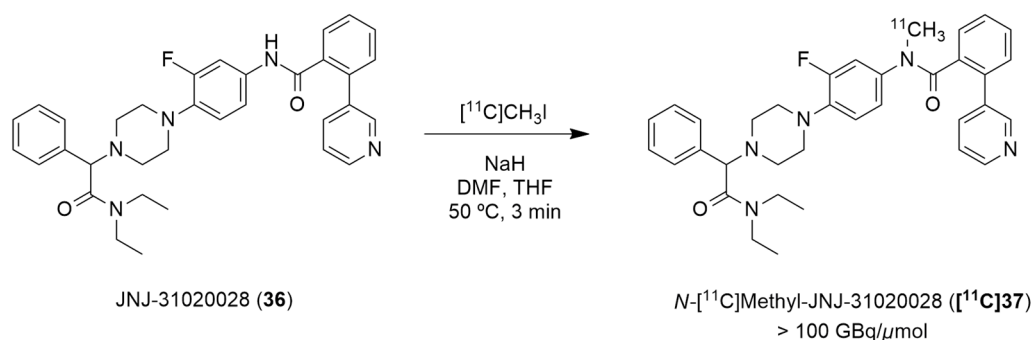


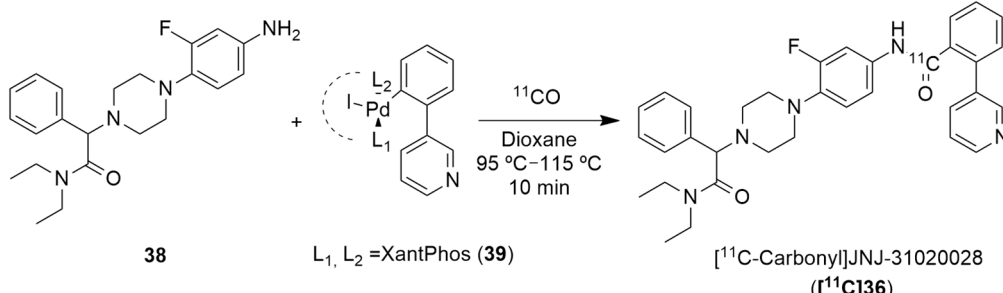
Figure 11. Radiosynthesis of *N*-[^{11}C]methyl-JNJ-31020028 ($[^{11}\text{C}]\mathbf{37}$).

The novel PET tracer [$^{11}\text{C}]\mathbf{37}$ was then assessed by the use of autoradiography in brain sections and by the *in vivo* PET imaging of the pig brain. The radiographic results have demonstrated that high densities of [$^{11}\text{C}]\mathbf{37}$ were found in the hippocampus and cerebellum, this is a finding which agrees with the anatomical distribution of the Y_2 receptors that has been described in other animal species. The radiotracer [$^{11}\text{C}]\mathbf{37}$ was also shown to be distributed rapidly into the brain and metabolized slowly in the bloodstream. The authors also concluded that PET studies using cyclosporine improved the target-to-background ratio of [$^{11}\text{C}]\mathbf{37}$, enabling the estimation of the pharmacokinetic parameters. This is due to the inhibition of the efflux transporter P-gp by cyclosporine as PET studies without cyclosporine gave a value of less than 1 for the ratio between the area under the whole-brain time–activity curve and the plasma time–activity curve of the radiotracer [$^{11}\text{C}]\mathbf{37}$, suggesting efflux transport at the blood–brain barrier [135].

Furthermore, Andersen et al. described the [^{11}C]carbonyl labeling of the same compound, JNJ-31020028 (**36**), by using palladium-aryl oxidative addition complexes in carbonylation reactions with [^{11}C]carbon monoxide [136]. [^{11}C -Carbonyl]JNJ-31020028 ($[^{11}\text{C}]\mathbf{36}$) was achieved with the best radiochemical yield of 25% (Table 5) and radiochemical purity of 55%, when the reaction of the amino precursor **38** was undertaken with the XantPhos ligated aryl palladium complex **39** and guanidine base Me-TDB (6 equiv.) in dioxane, at 95 °C for 10 min. To this end, the uses of different bases and ligated aryl palladium complexes and their correspondents ^{11}CO trapping efficiency and [$^{11}\text{C}]\mathbf{36}$ radiochemical purity and yield were evaluated. In a first attempt, when NEt₃ (1 equiv.) was added to the reaction of the amino precursor **38** with PPh₃ ligated aryl palladium complex, no traces of ^{11}CO trapping were observed (Table 5, entry 1). The implementation of the XantPhos ligated aryl palladium complex allowed the formation of the desired product [$^{11}\text{C}]\mathbf{36}$, though with low radiochemical yield, when DBU (4 equiv.) was used in the reaction (Table 5, entry 2). An increase in the reaction temperature led to a higher ^{11}CO trapping efficiency but lower radiochemical purity of the product (Table 5, entry 3). A series of different organobases were also tested. The use of DBN, proton-sponge and TMGN bases (4 equiv.) led to a low level of ^{11}CO gas trapping (Table 5, entries 4–6); however, the use of the guanidine base Me-TDB (4 equiv.) increased the reactivity profoundly and significantly higher values for the trapping efficiency and radiochemical purity of the product were observed (Table 5, entry 7). The augmentation of the temperature of the reaction did not have a beneficial

impact (Table 5, entry 8). Finally, the increase in the guanidine base amount to 6 equivalents led to the formation of [^{11}C -carbonyl]JNJ-31020028 ([^{11}C]36) with a good purity profile and acceptable radiochemical yield on an average of three reproducible reactions (Table 5, entry 9).

Table 5. Compound JNJ-31020028 [^{11}C]-Carbonyl labeling.



Entry	Complex	Base	Trapping Efficiency (%)	Radiochemical Purity (%)	Radiochemical Yield (%)
1	$L_1 = L_2 = \text{PPh}_3$	TEA	-	-	-
2 ^a	39	DBU	16	23	4
3 ^b	39	DBU	36	10	4
4	39	DBN	15	3	0.5
5	39	Proton-sponge	6	-	-
6	39	TMGN	22	-	-
7	39	Me-TDB	38	55	21
8 ^c	39	Me-TDB	42	25	11
9	39	Me-TDB	48 ± 7	55 ± 7	25 ± 4 (n = 3)

^a 90 °C; ^b 100 °C; ^c 115 °C

4.3. NPY Y₅ Receptor

In the literature, the first reported research using a PET ligand for the Y₅ receptor, performed by Eröndu et al. [42], aimed to test if NPY Y₅ antagonism would lead to weight loss in overweight and obese patients. In order to verify this hypothesis, MK-0557 [42] (**40**, Figure 12), a potent selective and orally available Y₅ antagonist, was used. In this case, these PET studies were aimed at providing complementary data about the MK-0557 dosage by studying the Y₅ receptor occupancy after the oral administration of **40**. The selective Y₅ PET ligand [^{11}C]MK-0233 ([^{11}C]41), which had been developed and validated in the rhesus monkey [137], was used in human volunteers. [^{11}C]41 has a similar structure to the Y₅ antagonist **40** and it is also extremely selective to this receptor (Figure 12). The long-term weight loss study with MK-0557 showed that, even though this NPY Y₅ antagonist had a favorable clinical safety profile, the magnitude of the induced weight loss was not clinically meaningful as the degree of weight loss after 52 weeks of treatment with **40** was significantly less compared to other weight loss drugs, the report showed [42]. These clinical studies provided a better clarification of the role of the NPY Y₅ receptor in human energy homeostasis and its utility as a target for anti-obesity drug therapy. The authors also concluded that, for the purposes of future anti-obesity drug development programs, targeting only the NPY Y₅ receptor was unlikely to produce therapeutic efficacy [42].

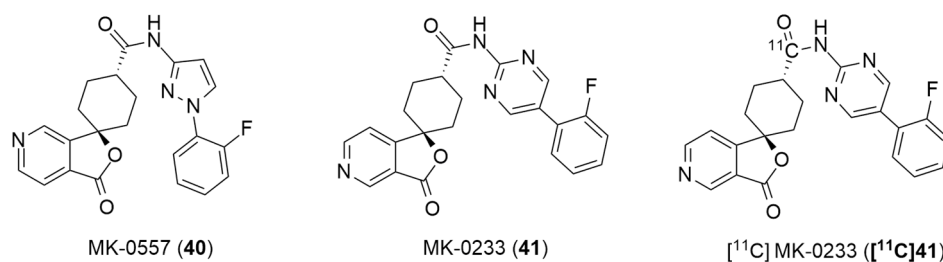


Figure 12. Structures of MK-0557 (40), MK-0233(41) and PET ligand $[^{11}\text{C}]$ MK-0233 ($[^{11}\text{C}]$ 41).

The synthesis and radiolabeling of compound 41 with $[^{11}\text{C}]$ was later published by Takahashi et al. [138]. The authors reported a series of *trans*-3-oxospiro[(aza)isobenzofuran-1(3*H*),1'-cyclohexane]-4'-carboxamide derivatives and examined their binding affinities towards the Y_5 receptor and their brain penetrability. Compound 41 showed the most promising biological profile for becoming a Y_5 PET tracer as it had a good Y_5 binding affinity of 1.5 ± 0.3 , an acceptable Log *P* value of 2.79 and was selective to the Y_5 receptor (human Y_1 , Y_2 and Y_4 $\text{IC}_{50} > 10 \mu\text{m}$). Moreover, its susceptibility to human and mouse P-glycoprotein transporters was studied and it was concluded that the precursor 41 was not a substrate of the human P-gp transporter. Thus, compound 41 was selected to be radiolabeled with $[^{11}\text{C}]$ in order to become a novel Y_5 PET tracer. Succinctly, the synthesis of 41 starts with the reaction of 3-bromopyridine 42 with LDA followed by 1,4-cyclohexanedione monoethyleneketal and acid mediated hydrolysis so as to obtain the ketone 43 (Figure 13). This was then stereoselectively reduced by NaBH_4 , providing the *cis*-alcohol 44. The *trans* carboxylic acid 45 was achieved by the mesylation of alcohol 44, followed by the reaction with NEt_4CN and acid mediated hydrolysis. Compound 45 was then coupled with 2-amino-5-*o*-fluorophenylpyrimidine in order to afford the precursor 46. The subsequent radiolabeling of precursor 46 can then be achieved by its reaction with $[^{11}\text{C}]\text{CO}$ in the presence of $\text{Pd}(\text{PPh}_3)_4$, providing $[^{11}\text{C}]$ 41 as a product [137,138]. No statements of the yield or molar activity of the radiolabeled product were disclosed.

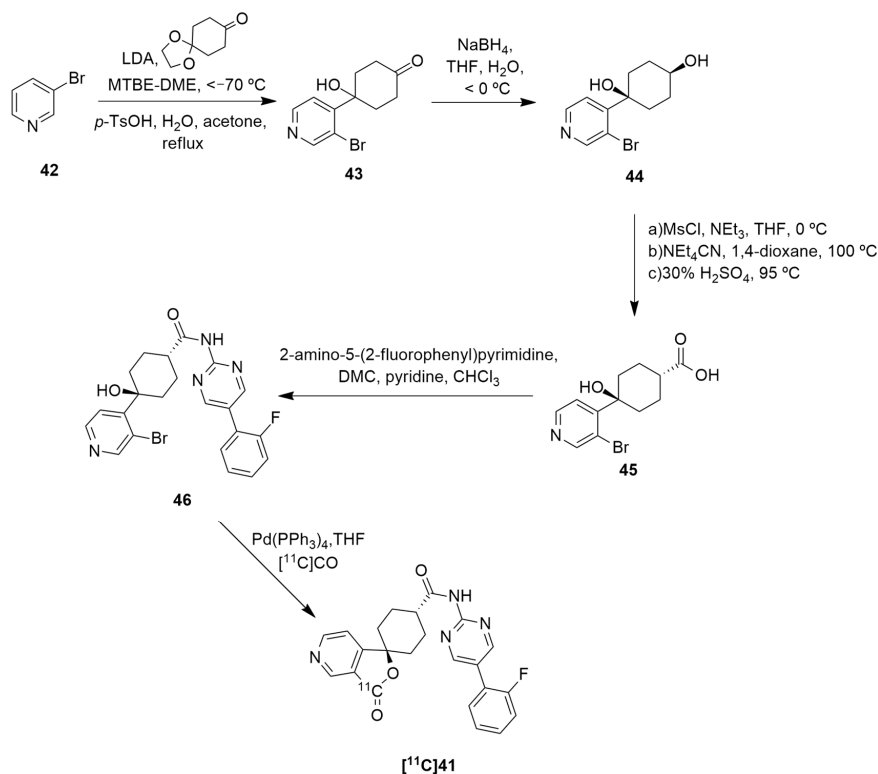


Figure 13. Synthetic route of precursor 46 and radiosynthesis of $[^{11}\text{C}]$ 41.

Afterwards, Kealey et al. reported the [^{11}C]carbonylation reaction of [^{11}C]41 using microfluidic technology [139]. The authors sought to enhance the reactivity of [^{11}C]CO by improving its solubility via chemical complexation to CO-binding molecules in a solution. They were able to achieve this by forming a copper [^{11}C]carbonyl complex, copper(I)tris(3,5-dimethylpyrazolyl)borate-[^{11}C]carbonyl ($\text{Cu}(\text{Tp}^*)[^{11}\text{C}]\text{CO}$), which was then used in the [^{11}C]carbonylation reaction that led to the formation of the radiolabeled compound [^{11}C]41. Hence, the radiosynthesis of [^{11}C]41 was produced through the ring-closing [^{11}C]carbonylation reaction between pyridyl-bromide and the hydroxyl functional groups of the precursor 46 and mediated by the catalyst $\text{Pd}(\text{PPh}_3)_4$. In this work, the authors synthesized [^{11}C]41 in two different ways: one using a microfluidic methodology and one using a low-pressure technique. Regarding the first method, the authors analyzed the temperature and flow rate's influence on the radiolabeling reaction and, so as to maximize the yields and minimize the synthesis reaction time that were required in order to obtain enough radiotracer [^{11}C]41 to perform the PET studies, the reactions were performed at 180°C with a flow rate of $100\ \mu\text{L}/\text{min}$. This led to the production of [^{11}C]MK-0233 with a molar activity of $100 \pm 30\ \text{GBq}/\mu\text{mol}$, radiochemical purity $> 99\%$ and a decay-corrected radiochemical yield of $7.2 \pm 0.7\%$ in 27 min of synthesis time. Concerning the second method, a 3 mL vial was used as the reaction vessel and, despite some problems and subsequent optimizations related to the apparatus, the radiolabeled compound was achieved with a molar activity of $100 \pm 15\ \text{GBq}/\mu\text{mol}$, radiochemical purity $> 99\%$ and a decay-corrected radiochemical yield of $7.1 \pm 2.2\%$, also in 27 min. The authors had initially predicted a greater difference between the results of these methods, but the radiochemical yields were almost identical and they were produced in the same amount of time. Nevertheless, the feasibility of using microfluidics for solutions-based carbonylations proved it to be a suitable method for PET tracers' production, with the potential to surpass the vial method.

More recently, Kumar et al. reported the identification and radiolabeling of four potent and selective Y_5 receptor antagonists that could emerge as Y_5 receptor PET tracers. The selected four candidates (47, 48, 49 and 50, Figure 14) showed high affinities towards the receptor and were suitable for radiolabeling with [^{18}F]fluoride via nucleophilic substitution reactions [140].

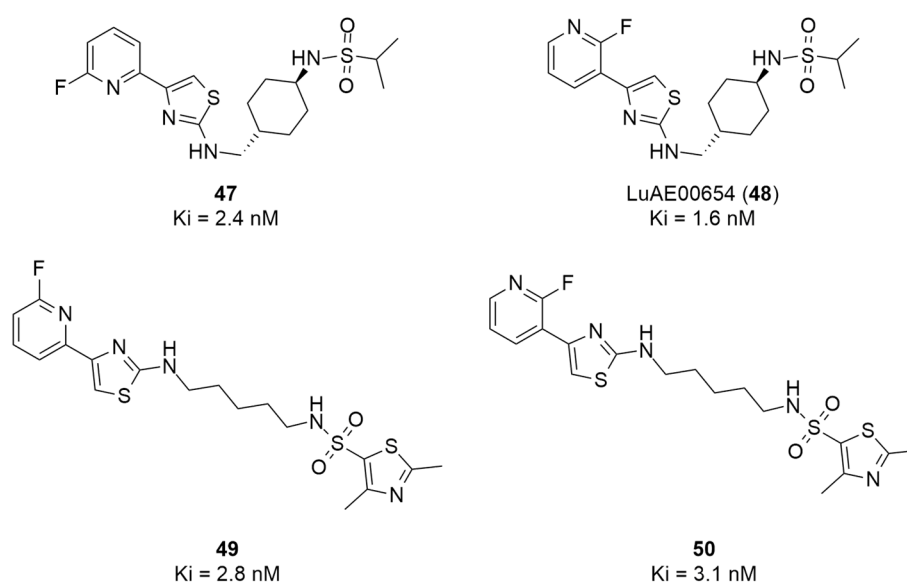


Figure 14. Selected candidate PET ligands for the Y_5 receptor.

The authors performed the non-radiolabeling experiments using KF/krytofix/K₂CO₃ in DMSO at 180 °C. Regarding the radiolabeling experiments, both conventional heating and microwave irradiation were tested. The radiolabeling of the compound **47** did not provide any radiolabeled product under conventional heating, although under microwave irradiation [¹⁸F]**47** was obtained in <2% isolated RCY (Table 6). The same results were obtained when radiolabeling compound **49**. [¹⁸F]LuAE00654 ([¹⁸F]**48**) was obtained with isolated RCY of 10 ± 4% and the radiolabeling of compound **50** produced [¹⁸F]**50** with 25 ± 5% RCY under microwave irradiation and 15 ± 3% RCY under conventional heating conditions. The radiochemical purities of the obtained radiolabeled products were >95% with an average molar activity of 2.5 ± 1% Ci/μmol. Given these results, PET studies were performed with the 2-substituted pyridyl thiazoles [¹⁸F]LuAE00654 ([¹⁸F]**48**) and [¹⁸F]**50** as they achieved better radiochemical yields than 6-substituted pyridyl thiazoles. The PET studies were carried out in fasted adult male baboons (*Papio anubis*). [¹⁸F]**48** showed good BBB penetration and was retained in several brain regions such as the caudate, putamen and cortical regions. The distribution of this radiotracer was shown to be compliant with the acknowledged distribution of the Y₅ receptor and [¹¹C]MK0233 in monkeys and human subjects. [¹⁸F]LuAE00654 also demonstrated itself to be of rapid clearance and its specificity was proven by blocking experiments using the Y₅ ligand LuA44608. Concerning the radiotracer [¹⁸F]**50**, even though it penetrated the baboons' blood–brain barriers, it showed little retention of radioactivity in the brain, fast washout and a faster metabolization in comparison to [¹⁸F]LuAE00654 ([¹⁸F]**48**). Thus, [¹⁸F]LuAE00654 ([¹⁸F]**48**) showed great promise as a PET radiotracer for the Y₅ receptor and could be used for the development of novel drugs aiming at the NPY Y₅ receptor functions.

Table 6. Radiosynthesis of NPY Y₅ ligands under microwave irradiation.

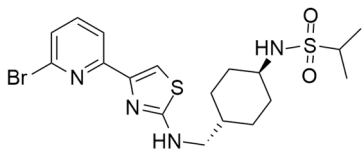
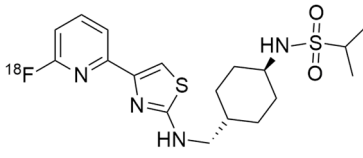
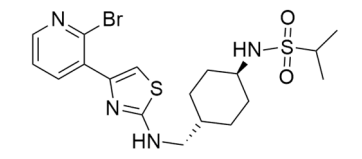
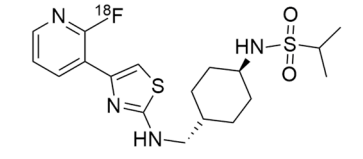
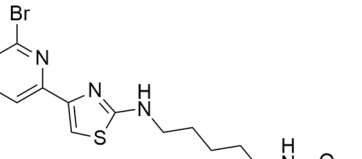
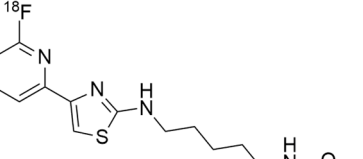
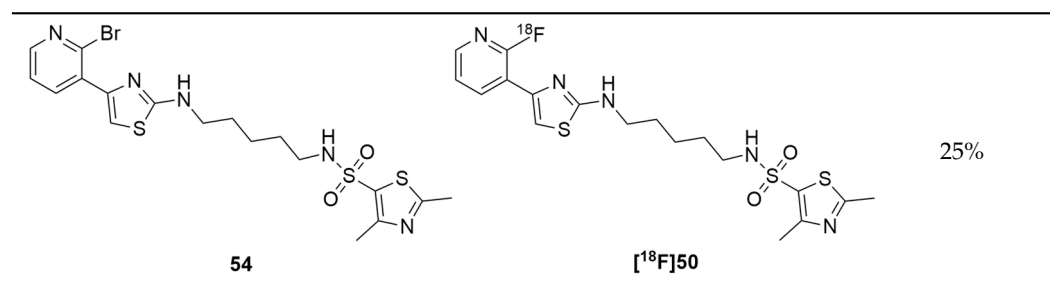
Precursors 51, 52, 53, 54		1. [¹⁸ F]KF/krytofix/K ₂ CO ₃ 2. DMSO, MW 3. HPLC purification	Radiolabeled products [¹⁸F]47, [¹⁸F]48, [¹⁸F]49, [¹⁸F]50		
Precursor			Radiolabeled Product	RCY	
	51			[¹⁸F]47	<2%
	52			[¹⁸F]LuAE00654 ([¹⁸F]48)	10%
	53			[¹⁸F]49	<2%

Table 6. Cont.



5. Conclusions

NPY has gained a lot of interest from the scientific community over the years and has been broadly studied and biologically and pharmacologically characterized due to its involvement in the pathophysiology of several diseases, especially brain diseases. To further understand its functioning, PET imaging of the NPY receptors has been investigated. For that purpose, several radiotracers were developed for three of the NPY receptors (Y_1 , Y_2 and Y_5). In this paper, we have highlighted some approaches to the chemical and radiolabeling development of the different radiotracers for the NPY receptors and the subsequent PET studies and results, which were mainly used in tumor visualization and receptor visualization associated with obesity and other hypothalamic disorders.

Despite the promising results that have been obtained so far with the pre-clinical and clinical studies, which were crucial to the better understanding of the NPY receptors in the several pathologies, it is clear that further investigation is still needed. The advances in NPY system PET imaging have been occurring at a slower rate as there is still some difficulty in not only developing novel radiotracers that combine good radiolabeling methods with good pharmacological profiles but also in expanding the preclinical development to the clinical area. Nevertheless, PET imaging of the NPY system holds a lot of potential to further the developments in and insights into this topic and to support the discovery and development of new promising CNS drugs that are able to target this important family of receptors in the years to come.

Author Contributions: I.C.F.F. wrote the manuscript. M.C.-B., C.C. and A.J.A. reviewed the manuscript to the final form. All authors have read and agreed to the published version of the manuscript.

Funding: The authors wish to thank the financial support from Portuguese National Funds via FCT—Fundação para a Ciência e a Tecnologia-UIDB/04539/2020, UIDP/04539/2020, UIDB/4950/2020, UIDP/4950/2020 and LA/P/0058/2020. Inês C. F. Fonseca also thanks FCT and ICNAS Pharma for her PhD grant PD/BDE/150334/2019.

Acknowledgments: Not applicable.

Conflicts of Interest: The authors declare no conflict of interest.

Abbreviations

NPY	Neuropeptide Y
PET	Positron emission tomography
CNS	Central nervous system
CT	Computerized tomography
MRI	Magnetic resonance imaging
SPECT	Single photon emission computed tomography
¹¹ C	Carbon-11
¹³ N	Nitrogen-13
¹⁸ F	Fluorine-18
⁶⁸ Ga	Galium-68

⁶⁴ Cu	Copper-64
¹²³ I	Iodine-123
^{99m} Tc	Technetium-99m
¹¹¹ In	Indium-111
⁶⁷ Ga	Galium-67
PYY	Peptide YY
PP	Pancreatic peptide
cAMP	Cyclic adenosine monophosphate
P-gp	P-glycoprotein
BBB	Blood–brain barrier
IC ₅₀	Half-maximal inhibitory concentration
SAR	Structure–activity relationship
K ₂₂₂	Kriptofix 222
DMSO	Dimethyl sulfoxide
HCl	Hydrochloric acid
HPLC	High performance liquid chromatography
THPTA	Tris(hydroxypropyltriazolylmethyl)amine
ACN	Acetonitrile
RAY	Radioactivity yield
DMF	<i>N,N</i> -dimethylformamide
EOI	End of irradiation
THF	Tetrahydrofuran
BCPR	Breast cancer resistance protein
HBPLs	Heterobivalent peptidic ligands
GRPR	Gastrin-releasing peptide receptor
TEA	Triethanolamine
DBU	1,8-Diazabicyclo[5,4,0]undec-7-ene
DBN	1,5-Diazabicyclo(4.3.0)non-5-ene
MTBE	Methyl tert-butyl ether
DME	Dimethoxyethane
DMC	Dimethyl carbonate
RCY	Radiochemical yield
MW	Microwave irradiation

References

1. Hammoud, D.A.; Hoffman, J.M.; Pomper, M.G. Molecular Neuroimaging: From Conventional to Emerging Techniques. *Radiology* **2007**, *245*, 21–42. [[CrossRef](#)] [[PubMed](#)]
2. Hargreaves, R.; Wagner, J.A. Imaging as Biomarker for Decision-Making in Drug Development. In *In Vivo MR Techniques in Drug Discovery and Development*, 1st ed.; Beckmann, N., Ed.; Taylor & Francis: New York, NY, USA, 2006; pp. 31–44.
3. Beckmann, N.; Rudin, M. The Drug Discovery and Development Process: Opportunities and Challenges for MR Techniques. In *In Vivo MR Techniques in Drug Discovery and Development*, 1st ed.; Beckmann, N., Ed.; Taylor & Francis: New York, NY, USA, 2006; pp. 7–29.
4. Filippi, M. (Ed.) *Oxford Textbook of Neuroimaging*, 1st ed.; Oxford University Press: Oxford, UK, 2015; pp. 3–96.
5. Rodie, M.E.; Forbes, K.P.; Muir, K. Advances in neuroimaging. *Endocr. Dev.* **2014**, *27*, 63–75. [[CrossRef](#)] [[PubMed](#)]
6. Hargreaves, R.J.; Rabiner, E.A. Translational PET imaging research. *Neurobiol. Dis.* **2014**, *61*, 32–38. [[CrossRef](#)]
7. Fischman, A.J.; Alpert, N.M.; Rubin, R.H. Pharmacokinetic Imaging—A Noninvasive Method for Determining Drug Distribution and Action. *Clin. Pharmacokinet.* **2002**, *41*, 581–602. [[CrossRef](#)]
8. Rudin, M.; Weissleder, R. Molecular imaging in drug discovery and development. *Nat. Rev. Drug Discov.* **2003**, *2*, 123–131. [[CrossRef](#)] [[PubMed](#)]
9. Matthews, P.M.; Rabiner, E.A.; Passchier, J.; Gunn, R.N. Positron emission tomography molecular imaging for drug development. *Br. J. Clin. Pharmacol.* **2012**, *73*, 175–186. [[CrossRef](#)]
10. Cherry, S.R.; Dahlbom, M. PET: Physics, Instrumentation, and Scanners. In *PET: Molecular Imaging and Its Biological Applications*; Phelps, M.E., Ed.; Springer: New York, NY, USA, 2004; pp. 1–124. [[CrossRef](#)]
11. Cherry, S.R. Fundamentals of Positron Emission Tomography and Applications in Preclinical Drug Development. *J. Clin. Pharmacol.* **2001**, *41*, 482–491. [[CrossRef](#)]
12. Cherry, S.R.; Gambhir, S.S. Use of positron emission tomography in animal research. *ILAR J.* **2001**, *42*, 219–232. [[CrossRef](#)]
13. Jones, T.; Rabiner, E.A. The development, past achievements, and future directions of brain PET. *J. Cereb. Blood Flow Metab.* **2012**, *32*, 1426–1454. [[CrossRef](#)]

14. Brothers, S.P.; Wahlestedt, C. Therapeutic potential of neuropeptide Y (NPY) receptor ligands. *EMBO Mol. Med.* **2010**, *2*, 429–439. [[CrossRef](#)]
15. Reichmann, F.; Holzer, P. Neuropeptide Y: A stressful review. *Neuropeptides* **2016**, *55*, 99–109. [[CrossRef](#)] [[PubMed](#)]
16. Santos-Carvalho, A.; Álvaro, A.R.; Martins, J.; Ambrósio, A.F.; Cavadas, C. Emerging novel roles of neuropeptide Y in the retina: From neuromodulation to neuroprotection. *Prog. Neurobiol.* **2014**, *112*, 70–79. [[CrossRef](#)] [[PubMed](#)]
17. Duarte-Neves, J.; Pereira de Almeida, L.; Cavadas, C. Neuropeptide Y (NPY) as a therapeutic target for neurodegenerative diseases. *Neurobiol. Dis.* **2016**, *95*, 210–224. [[CrossRef](#)] [[PubMed](#)]
18. Silva, A.P.; Cavadas, C.; Grouzmann, E. Neuropeptide Y and its receptors as potential therapeutic drug targets. *Clin. Chim. Acta* **2002**, *326*, 3–25. [[CrossRef](#)]
19. Zhang, L.; Bijker, M.S.; Herzog, H. The neuropeptide Y system: Pathophysiological and therapeutic implications in obesity and cancer. *Pharmacol. Ther.* **2011**, *131*, 91–113. [[CrossRef](#)]
20. Page, M.J.; McKenzie, J.E.; Bossuyt, P.M.; Boutron, I.; Hoffmann, T.C.; Mulrow, C.D.; Shamseer, L.; Tetzlaff, J.M.; Akl, E.A.; Brennan, S.E.; et al. The PRISMA 2020 statement: An updated guideline for reporting systematic reviews. *BMJ.* **2021**, *372*, n71. [[CrossRef](#)]
21. Tatemoto, K.; Carlsquist, M.; Mutt, V. Neuropeptide Y—A novel brain peptide with structural similarities to peptide YY and pancreatic polypeptide. *Nature* **1982**, *296*, 659–660. [[CrossRef](#)]
22. Larhammar, D. Evolution of neuropeptide Y, peptide YY and pancreatic polypeptide. *Regul. Pept.* **1996**, *62*, 1–11. [[CrossRef](#)]
23. Tatemoto, K. Neuropeptide Y: Complete amino acid sequence of the brain peptide. *Proc. Natl. Acad. Sci. USA* **1982**, *79*, 5485–5489. [[CrossRef](#)]
24. Fuhlendorff, J.; Johansen, N.L.; Melberg, S.G.; Thøgersen, H.; Schwartz, T.W. The antiparallel pancreatic polypeptide fold in the binding of neuropeptide Y to Y₁ and Y₂ receptors. *J. Biol. Chem.* **1990**, *265*, 11706–11712. [[CrossRef](#)]
25. Naruse, S.; Kitagawa, M.; Ishiguro, H.; Hayakawa, T. Feedback regulation of pancreatic secretion by peptide YY. *Peptides* **2002**, *23*, 359–365. [[CrossRef](#)]
26. Fujimiya, M.; Inui, A. Peptidergic regulation of gastrointestinal motility in rodents. *Peptides* **2000**, *21*, 1565–1582. [[CrossRef](#)]
27. Batterham, R.L.; Cowley, M.A.; Small, C.J.; Herzog, H.; Cohen, M.A.; Dakin, C.L.; Wren, A.M.; Brynes, A.E.; Low, M.J.; Ghatei, M.A.; et al. Gut hormone PYY₃₋₃₆ physiologically inhibits food intake. *Nature* **2002**, *418*, 650–654. [[CrossRef](#)] [[PubMed](#)]
28. Hazelwood, R.L. The Pancreatic Polypeptide (PP-Fold) Family: Gastrointestinal, Vascular, and Feeding Behavioral Implications. *Proc. Soc. Exp. Biol. Med.* **1993**, *202*, 44–63. [[CrossRef](#)]
29. Batterham, R.L.; Le Roux, C.W.; Cohen, M.A.; Park, A.J.; Ellis, S.M.; Patterson, M.; Frost, G.S.; Ghatei, M.A.; Bloom, S.R. Pancreatic polypeptide reduces appetite and food intake in humans. *J. Clin. Endocrinol. Metab.* **2003**, *88*, 3989–3992. [[CrossRef](#)]
30. Adrian, T.E.; Allen, J.M.; Bloom, S.R.; Ghatei, M.A.; Rossor, M.N.; Roberts, G.W.; Crow, T.J.; Tatemoto, K.; Polak, J.M. Neuropeptide Y distribution in human brain. *Nature* **1983**, *306*, 584–586. [[CrossRef](#)]
31. Allen, Y.S.; Adrian, T.E.; Allen, J.M.; Tatemoto, K.; Crow, T.J.; Bloom, S.R.; Polak, J.M. Neuropeptide Y Distribution in the Rat Brain. *Science* **1983**, *221*, 877–879. [[CrossRef](#)]
32. Sundler, F.; Böttcher, G.; Ekblad, E.; Hakanson, R. PP, PYY, and NPY, Occurrence and Distribution in the Periphery. In *The Biology of Neuropeptide Y and Related Peptides*; Colmers, W.F., Wahlestedt, C., Eds.; Humana Press: Totowa, NJ, USA, 1993; pp. 157–196. [[CrossRef](#)]
33. Michel, M.C.; Beck-Sickinger, A.; Cox, H.; Doods, H.N.; Herzog, H.; Larhammar, D.; Quirion, R.; Schwartz, T.; Westfall, T. XVI. International Union of Pharmacology Recommendations for the Nomenclature of Neuropeptide Y, Peptide YY, and Pancreatic Polypeptide Receptors. *Pharmacol. Rev.* **1998**, *50*, 143–150.
34. Lee, C.C.; Miller, R.J. Is there really an NPY Y₃ receptor? *Regul. Pept.* **1998**, *75–76*, 71–78. [[CrossRef](#)]
35. Rudolf, K.; Eberlein, W.; Engel, W.; Wieland, H.A.; Willim, K.D.; Entzeroth, M.; Wienen, W.; Beck-Sickinger, A.G.; Doods, H.N. The first highly potent and selective non-peptide neuropeptide Y Y₁ receptor antagonist: BIBP3226. *Eur. J. Pharmacol.* **1994**, *271*, R11–R13. [[CrossRef](#)]
36. King, P.J.; Widdowson, P.S.; Doods, H.N.; Williams, G. Regulation of Neuropeptide Y Release by Neuropeptide Y Receptor Ligands and Calcium Channel Antagonists in Hypothalamic Slices. *J. Neurochem.* **1999**, *73*, 641–646. [[CrossRef](#)] [[PubMed](#)]
37. Parker, R.M.; Herzog, H. Regional distribution of Y-receptor subtype mRNAs in rat brain. *Eur. J. Neurosci.* **1999**, *11*, 1431–1448. [[CrossRef](#)] [[PubMed](#)]
38. Balasubramaniam, A.; Mullins, D.E.; Lin, S.; Zhai, W.; Tao, Z.; Dhawan, V.C.; Guzzi, M.; Knittel, J.J.; Slack, K.; Herzog, H.; et al. Neuropeptide Y (NPY) Y₄ Receptor Selective Agonists Based on NPY(32–36): Development of an Anorectic Y₄ Receptor Selective Agonist with Picomolar Affinity. *J. Med. Chem.* **2006**, *49*, 2661–2665. [[CrossRef](#)]
39. Li, J.-B.; Asakawa, A.; Terashi, M.; Chenga, K.; Chaolua, H.; Zoshiki, T.; Ushikai, M.; Sheriff, S.; Balasubramaniam, A.; Inui, A. Regulatory effects of Y₄ receptor agonist (BVD-74D) on food intake. *Peptides* **2010**, *31*, 1706–1710. [[CrossRef](#)] [[PubMed](#)]
40. Rodriguez, M.; Audinot, V.; Dromaint, S.; Macia, C.; Lamamy, V.; Beauverger, P.; Rique, H.; Imbert, J.; Nicolas, J.P.; Boutin, J.A.; et al. Molecular identification of the long isoform of the human neuropeptide Y Y₅ receptor and pharmacological comparison with the short Y₅ receptor isoform. *Biochem. J.* **2003**, *369*, 667–673. [[CrossRef](#)]
41. Gerald, C.; Walker, M.W.; Criscione, L.; Gustafson, E.L.; Batzl-Hartmann, C.; Smith, K.E.; Vaysse, P.; Durkin, M.M.; Laz, T.M.; Linemeyer, D.L.; et al. A receptor subtype involved in neuropeptide-Y-induced food intake. *Nature* **1996**, *382*, 168–171. [[CrossRef](#)]

42. Erondou, N.; Gantz, I.; Musser, B.; Suryawanshi, S.; Mallick, M.; Addy, C.; Cote, J.; Bray, G.; Fujioka, K.; Bays, H.; et al. Neuropeptide Y5 receptor antagonism does not induce clinically meaningful weight loss in overweight and obese adults. *Cell Metab.* **2006**, *4*, 275–282. [[CrossRef](#)]
43. Haga, Y.; Sakamoto, T.; Shibata, T.; Nonoshita, K.; Ishikawa, M.; Suga, T.; Takahashi, H.; Takahashi, T.; Takahashi, H.; Ando, M.; et al. Discovery of trans-N-[1-(2-fluorophenyl)-3-pyrazolyl]-3-oxospiro-[6-azaisobenzofuran-1(3H),10-cyclohexane]-40-carboxamide, a potent and orally active neuropeptide Y Y5 receptor antagonist. *Bioorg. Med. Chem.* **2009**, *17*, 6971–6982. [[CrossRef](#)]
44. Fuhendorff, J.; Gether, U.; Aakerlund, L.; Langeland-Johansen, N.; Thøgersen, H.; Melberg, S.G.; Olsen, U.B.; Thastrup, O.; Schwartz, T.W. [Leu31,Pro34]Neuropeptide Y: A specific Y1 receptor agonist. *Proc. Natl. Acad. Sci. USA* **1990**, *87*, 182–186. [[CrossRef](#)]
45. Dumont, Y.; Cadieux, A.; Pheng, L.-H.; Fournier, A.; St-Pierre, S.; Quirion, R. Peptide YY derivatives as selective neuropeptide Y/peptide YY Y1 and Y2 agonists devoided of activity for the Y3 receptor sub-type. *Brain Res. Mol. Brain Res.* **1994**, *26*, 320–324. [[CrossRef](#)]
46. Söll, R.M.; Dinger, M.C.; Lundell, I.; Larhammer, D.; Beck-Sickinge, A.G. Novel analogues of neuropeptide Y with a preference for the Y1-receptor. *Eur. J. Biochem.* **2001**, *268*, 2828–2837. [[CrossRef](#)] [[PubMed](#)]
47. Wieland, H.A.; Engel, W.; Eberlein, W.; Rudolf, K.; Doods, H.N. Subtype selectivity of the novel nonpeptide neuropeptide Y Y1 receptor antagonist BIBO 3304 and its effect on feeding in rodents. *Br. J. Pharmacol.* **1998**, *125*, 549–555. [[CrossRef](#)] [[PubMed](#)]
48. Serradeil-Le Gal, C.; Valette, G.; Rouby, P.; Pellet, A.; Oury-Donat, F.; Brossard, G.; Lespy, L.; Marty, E.; Neliat, G.; Cointet, P.; et al. SR120819A, an orally-active and selective neuropeptide Y Y1 receptor antagonist. *FEBS Lett.* **1995**, *362*, 192–196. [[CrossRef](#)]
49. Hipskind, P.A.; Lobb, K.L.; Nixon, J.A.; Britton, T.C.; Bruns, R.F.; Catlow, J.; Dieckman-McGinty, D.K.; Gackenhimer, S.L.; Gitter, B.D.; Iyengar, S.; et al. Potent and Selective 1,2,3-Trisubstituted Indole NPY Y-1 Antagonists. *J. Med. Chem.* **1997**, *40*, 3712–3714. [[CrossRef](#)] [[PubMed](#)]
50. Kanatani, A.; Hata, M.; Mashiko, S.; Ishihara, A.; Okamoto, O.; Haga, Y.; Ohe, T.; Kanno, T.; Murai, N.; Ishii, Y.; et al. A Typical Y1 Receptor Regulates Feeding Behaviors: Effects of a Potent and Selective Y1 Antagonist, J-115814. *Mol. Pharmacol.* **2001**, *59*, 501–505. [[CrossRef](#)]
51. Daniels, A.J.; Chance, W.T.; Grizzle, M.K.; Heyer, D.; Matthews, J.E. Food intake inhibition and reduction in body weight gain in rats treated with GI264879A, a non-selective NPY-Y1 receptor antagonist. *Peptides* **2001**, *22*, 483–491. [[CrossRef](#)]
52. Daniels, A.J.; Matthews, J.E.; Slepatis, R.J.; Jansen, M.; Viveros, O.H.; Tadepalli, A.; Harrington, W.; Heyer, D.; Landavazo, A.; Leban, J.J. High-affinity neuropeptide Y receptor antagonists. *Proc. Natl. Acad. Sci. USA* **1995**, *92*, 9067–9071. [[CrossRef](#)]
53. Malmström, R.E.; Balmér, K.C.; Weilitz, J.; Nordlander, M.; Sjölander, M. Pharmacology of H 394/84, a dihydropyridine neuropeptide Y Y1 receptor antagonist, in vivo. *Eur. J. Pharmacol.* **2001**, *418*, 95–104. [[CrossRef](#)]
54. Wright, J.; Bolton, G.; Creswell, M.; Downing, D.; Georgic, L.; Heffner, T.; Hodges, J.; MacKenzie, R.; Wise, L. 8-Amino-6-(Arylsulphonyl)-5-Nitroquinolines: Novel Nonpeptide Neuropeptide Y1 Receptor Antagonists. *Bioorg. Med. Chem. Lett.* **1996**, *6*, 1809–1814. [[CrossRef](#)]
55. Poindexter, G.S.; Bruce, M.A.; LeBoulluec, K.L.; Monkovic, I.; Martin, S.W.; Parker, E.M.; Iben, L.G.; McGovern, R.T.; Ortiz, A.A.; Stanley, J.A.; et al. Dihydropyridine Neuropeptide Y Y1 Receptor Antagonists. *Bioorg. Med. Chem. Lett.* **2002**, *12*, 379–382. [[CrossRef](#)]
56. Poindexter, G.S.; Bruce, M.A.; Breitenbucher, J.G.; Higgins, M.A.; Sit, S.-Y.; Romine, J.L.; Martin, S.W.; Ward, S.A.; McGovern, R.T.; Clarke, W.; et al. Dihydropyridine neuropeptide Y Y1 receptor antagonists 2: Bioisosteric urea replacements. *Bioorg. Med. Chem.* **2004**, *12*, 507–521. [[CrossRef](#)] [[PubMed](#)]
57. Kanatani, A.; Kanno, T.; Ishihara, A.; Hata, M.; Sakuraba, A.; Tanaka, T.; Tsuchiya, Y.; Mase, T.; Fukuroda, T.; Fukami, T.; et al. The Novel Neuropeptide Y Y1 Receptor Antagonist J-104870: A Potent Feeding Suppressant with Oral Bioavailability. *Biochem. Biophys. Res. Commun.* **1999**, *266*, 88–91. [[CrossRef](#)] [[PubMed](#)]
58. Balasubramaniam, A.; Dhawan, V.C.; Mullins, D.E.; Chance, W.T.; Sheriff, S.; Guzzi, M.; Prabhakaran, M.; Parker, E.M. Highly selective and potent neuropeptide Y (NPY) Y1 receptor antagonists based on [Pro(30), Tyr(32), Leu(34)]NPY(28-36)-NH2 (BW1911U90). *J. Med. Chem.* **2001**, *44*, 1479–1482. [[CrossRef](#)] [[PubMed](#)]
59. Balasubramaniam, A.; Zhai, W.; Sheriff, S.; Tao, Z.; Chance, W.T.; Fischer, J.E.; Eden, P.; Taylor, J. Bis(31/31′)[[Cys(31),Trp(32),Nva(34)] NPY-(31-36)]: A Specific NPY Y-1 Receptor Antagonist. *J. Med. Chem.* **1996**, *39*, 811–813. [[CrossRef](#)] [[PubMed](#)]
60. Balasubramaniam, A.; Ujhelyi, M.; Borchers, M.; Huang, Y.; Zhai, W.; Zhou, Y.; Johnson, M.; Sheriff, S.; Fischer, J.E. Antagonistic properties of centrally truncated analogs of [D-Trp(32)]NPY. *J. Med. Chem.* **1996**, *39*, 1142–1147. [[CrossRef](#)]
61. Kishi, T.; Aschkenasi, C.J.; Choi, B.J.; Lopez, M.E.; Lee, C.E.; Liu, H.; Hollenberg, A.N.; Friedman, J.M.; Elmquist, J.K. Neuropeptide Y Y1 Receptor mRNA in Rodent Brain: Distribution and Colocalization with Melanocortin-4 Receptor. *J. Comp. Neurol.* **2005**, *482*, 217–243. [[CrossRef](#)]
62. Kanatani, A.; Mashiko, S.; Murai, N.; Sugimoto, N.; Ito, J.; Fukuroda, T.; Fukami, T.; Morin, N.; MacNeil, D.J.; Van der Ploeg, L.H.; et al. Role of the Y1 Receptor in the Regulation of Neuropeptide Y-Mediated Feeding: Comparison of Wild-Type, Y1 Receptor-Deficient, and Y5 Receptor-Deficient Mice. *Endocrinology* **2000**, *141*, 1011–1016. [[CrossRef](#)]
63. Kask, A.; Rågo, L.; Harro, J. Evidence for involvement of neuropeptide Y receptors in the regulation of food intake: Studies with Y₁-selective antagonist BIBP3226. *Br. J. Pharmacol.* **1998**, *124*, 1507–1515. [[CrossRef](#)]

64. Naveilhan, P.; Hassani, H.; Lucas, G.; Blakeman, K.H.; Hao, J.-X.; Xu, X.-J.; Wiesenfeld-Hallin, Z.; Thorén, P.; Ernfors, P. Reduced antinociception and plasma extravasation in mice lacking a neuropeptide Y receptor. *Nature* **2001**, *409*, 513–517. [[CrossRef](#)]
65. Kalra, S.P.; Fuentes, M.; Fournier, A.; Parker, S.L.; Crowley, W.R. Involvement of the Y-1 receptor subtype in the regulation of luteinizing hormone secretion by neuropeptide Y in rats. *Endocrinology* **1992**, *130*, 3323–3330. [[CrossRef](#)]
66. Thiele, T.E.; Koh, M.T.; Pedrazzini, T. Voluntary Alcohol Consumption Is Controlled via the Neuropeptide Y Y1 Receptor. *J. Neurosci.* **2002**, *22*, RC208:1–RC208:6. [[CrossRef](#)]
67. Schroeder, J.P.; Olive, F.; Koenig, H.; Hodge, C.W. Intra-Amygdala Infusion of the NPY Y1 Receptor Antagonist BIBP 3226 Attenuates Operant Ethanol Self-Administration. *Alcohol. Clin. Exp. Res.* **2003**, *27*, 1884–1891. [[CrossRef](#)] [[PubMed](#)]
68. Sparta, D.R.; Fee, J.R.; Hayes, D.M.; Knapp, D.J.; MacNeil, D.J.; Thiele, T.E. Peripheral and Central Administration of a Selective Neuropeptide Y Y1 Receptor Antagonist Suppresses Ethanol Intake by C57BL/6J Mice. *Alcohol. Clin. Exp. Res.* **2004**, *28*, 1324–1330. [[CrossRef](#)] [[PubMed](#)]
69. Broqua, P.; Wettstein, J.G.; Rocher, M.N.; Gauthier-Martin, B.; Junien, J.L. Behavioral effects of neuropeptide Y receptor agonists in the elevated plus-maze and fear-potentiated startle procedures. *Behav. Pharmacol.* **1995**, *6*, 215–222. [[CrossRef](#)] [[PubMed](#)]
70. Heilig, M. Antisense inhibition of neuropeptide Y (NPY)-Y1 receptor expression blocks the anxiolytic-like action of NPY in amygdala and paradoxically increases feeding. *Regul. Pept.* **1995**, *59*, 201–205. [[CrossRef](#)]
71. Malis, D.-D.; Grouzmann, E.; Morel, D.R.; Mutter, M.; Lacroix, J.-S. Influence of TASP-V, a novel neuropeptide Y (NPY) Y₂ agonist, on nasal and bronchial responses evoked by histamine in anaesthetized pigs and in humans. *Br. J. Pharmacol.* **1999**, *126*, 989–996. [[CrossRef](#)] [[PubMed](#)]
72. Rist, B.; Zerbe, O.; Ingenhoven, N.; Scapozza, L.; Peers, C.; Vaughan, P.F.T.; McDonald, R.L.; Wieland, H.A.; Beck-Sickinger, A.G. Modified, cyclic dodecapeptide analog of neuropeptide Y is the smallest full agonist at the human Y₂ receptor. *FEBS Lett.* **1996**, *394*, 169–173. [[CrossRef](#)]
73. Grouzmann, E.; Buclin, T.; Martire, M.; Cannizzaro, C.; Dörner, B.; Razaname, A.; Mutter, M. Characterization of a selective antagonist of neuropeptide Y at the Y₂ receptor. Synthesis and pharmacological evaluation of a Y₂ antagonist. *J. Biol. Chem.* **1997**, *272*, 7699–7706. [[CrossRef](#)]
74. Doods, H.; Gaida, W.; Wieland, H.A.; Dollinger, H.; Schnorrenberg, G.; Esser, F.; Engel, W.; Eberlein, W.; Rudolf, K. BIIE0246: A selective and high affinity neuropeptide Y Y₂ receptor antagonist. *Eur. J. Pharmacol.* **1999**, *384*, R3–R5. [[CrossRef](#)]
75. Jablonowski, J.A.; Chai, W.; Li, X.; Rudolph, D.A.; Murray, W.V.; Youngman, M.A.; Dax, S.L.; Nepomuceno, D.; Bonaventure, P.; Lovenberg, T.W.; et al. Novel non-peptidic neuropeptide Y Y₂ receptor antagonists. *Bioorg. Med. Chem. Lett.* **2004**, *14*, 1239–1242. [[CrossRef](#)]
76. Shoblock, J.R.; Welty, N.; Nepomuceno, D.; Lord, B.; Aluisio, L.; Fraser, I.; Motley, S.T.; Sutton, S.W.; Morton, K.; Galici, R.; et al. In vitro and in vivo characterization of JNJ-31020028 (N-(4-{4-[2-(diethylamino)-2-oxo-1-phenylethyl]piperazin-1-yl}-3-fluorophenyl)-2-pyridin-3-ylbenzamide), a selective brain penetrant small molecule antagonist of the neuropeptide Y Y₂ receptor. *Psychopharmacology* **2010**, *208*, 265–277. [[CrossRef](#)] [[PubMed](#)]
77. Brothers, S.P.; Saldanha, S.A.; Spicer, T.P.; Cameron, M.; Mercer, B.A.; Chase, P.; McDonald, P.; Wahlestedt, C.; Hodder, P.S. Selective and Brain Penetrant Neuropeptide Y Y₂ Receptor Antagonists Discovered by Whole-Cell High-Throughput Screening. *Mol. Pharmacol.* **2009**, *77*, 46–57. [[CrossRef](#)] [[PubMed](#)]
78. Saldanha, S.A.; Brothers, S.P.; Spicer, T.; Cameron, M.; Mercer, B.A.; Chase, P.; McDonald, P.; Wahlestedt, C.; Hodder, P.S. Probe Report for NPY-Y₂ Receptor Antagonists. In *Probe Reports from the NIH Molecular Libraries Program*; National Center for Biotechnology Information (US): Bethesda, MD, USA, 2010.
79. Mittapalli, G.K.; Vellucci, D.; Yang, J.; Toussaint, M.; Brothers, S.P.; Wahlestedt, C.; Roberts, E. Synthesis and SAR of selective small molecule neuropeptide Y Y₂ receptor antagonists. *Bioorg. Med. Chem. Lett.* **2012**, *22*, 3916–3920. [[CrossRef](#)] [[PubMed](#)]
80. Lunniss, G.E.; Barnes, A.A.; Barton, N.; Biagetti, M.; Bianchi, F.; Blowers, S.M.; Caberlotto, L.; Emmons, A.; Holmes, I.P.; Montanari, D.; et al. The identification and optimisation of novel and selective diamide neuropeptide Y Y₂ receptor antagonists. *Bioorg. Med. Chem. Lett.* **2009**, *19*, 4022–4025. [[CrossRef](#)]
81. Lunniss, G.E.; Barnes, A.A.; Barton, N.; Biagetti, M.; Bianchi, F.; Blowers, S.M.; Caberlotto, L.L.; Emmons, A.; Holmes, I.P.; Montanari, D.; et al. The identification of a series of novel, soluble non-peptidic neuropeptide Y Y₂ receptor antagonists. *Bioorg. Med. Chem. Lett.* **2010**, *20*, 7341–7344. [[CrossRef](#)]
82. Pluym, N.; Baumeister, P.; Keller, M.; Bernhardt, G.; Buschauer, A. [(3)H]UR-PLN196: A Selective Nonpeptide Radioligand and Insurmountable Antagonist for the Neuropeptide Y Y₂ Receptor. *ChemMedChem* **2013**, *8*, 587–593. [[CrossRef](#)]
83. Dumont, Y.; Jacques, D.; Bouchard, P.; Quirion, R. Species Differences in the Expression and Distribution of the Neuropeptide Y Y₁, Y₂, Y₄, and Y₅ Receptors in Rodents, Guinea Pig, and Primates Brains. *J. Comp. Neurol.* **1998**, *402*, 372–384. [[CrossRef](#)]
84. Naveilhan, P.; Neveu, I.; Arenas, E.; Ernfors, P. Complementary and Overlapping Expression of Y₁, Y₂ And Y₅ Receptors In The Developing And Adult Mouse Nervous System. *Neuroscience* **1998**, *87*, 289–302. [[CrossRef](#)]
85. Babilon, S.; Mörl, K.; Beck-Sickinger, A.G. Towards improved receptor targeting: Anterograde transport, internalization and postendocytic trafficking of neuropeptide Y receptors. *Biol. Chem.* **2013**, *394*, 921–936. [[CrossRef](#)]
86. Parker, S.L.; Balasubramaniam, A. Neuropeptide Y Y₂ receptor in health and disease. *Br. J. Pharmacol.* **2008**, *153*, 420–431. [[CrossRef](#)]
87. Soscia, S.J.; Harrington, M.E. Neuropeptide Y does not reset the circadian clock in NPY Y₂-/- mice. *Neurosci. Lett.* **2005**, *373*, 175–178. [[CrossRef](#)] [[PubMed](#)]

88. Thorsell, A.; Rimondini, R.; Heilig, M. Blockade of central neuropeptide Y (NPY) Y2 receptors reduces ethanol self-administration in rats. *Neurosci. Lett.* **2002**, *332*, 1–4. [[CrossRef](#)]
89. Redrobe, J.P.; Dumont, Y.; Herzog, H.; Quirion, R. Characterization of Neuropeptide Y, Y₂ Receptor Knockout Mice in Two Animal Models of Learning and Memory Processing. *J. Mol. Neurosci.* **2004**, *22*, 159–166. [[CrossRef](#)]
90. Edelsbrunner, M.E.; Painsipp, E.; Herzog, H.; Holzer, P. Evidence from knockout mice for distinct implications of neuropeptide-Y Y2 and Y4 receptors in the circadian control of locomotion, exploration, water and food intake. *Neuropeptides* **2009**, *43*, 491–497. [[CrossRef](#)]
91. Monnet, F.P.; Fournier, A.; Debonnel, G.; de Montigny, C. Neuropeptide Y Potentiates Selectively the N-Methyl-D-Aspartate Response in the Rat CA3 Dorsal Hippocampus. I. Involvement of an Atypical Neuropeptide Y Receptor. *J. Pharmacol. Exp. Ther.* **1992**, *263*, 1212–1218.
92. Glaum, S.R.; Miller, R.J.; Rhim, H.; Maclean, D.; Georgic, L.M.; MacKenzie, R.G.; Grundemar, L. Characterization of Y3 receptor-mediated synaptic inhibition by chimeric neuropeptide Y-peptide YY peptides in the rat brainstem. *Br. J. Pharmacol.* **1997**, *120*, 481–487. [[CrossRef](#)]
93. Cavadas, C.; Silva, A.P.; Mosimann, F.; Cotrim, M.D.; Fontes Ribeiro, C.A.; Brunner, H.R.; Grouzmann, E. NPY Regulates Catecholamine Secretion from Human Adrenal Chromaffin Cells. *J. Clin. Endocrinol. Metab.* **2001**, *86*, 5956–5963. [[CrossRef](#)]
94. Schober, D.A.; Van Abbema, A.M.; Smiley, D.L.; Bruns, R.F.; Gehlert, D.R. The Neuropeptide Y Y₁ Antagonist, 1229U91, A Potent Agonist for the Human Pancreatic Polypeptide-Preferring (NPY Y4) Receptor. *Peptides* **1998**, *19*, 537–542. [[CrossRef](#)]
95. Parker, E.M.; Babij, C.K.; Balasubramaniam, A.; Burrier, R.E.; Guzzi, M.; Hamud, F.; Mukhopadhyay, G.; Rudinski, M.S.; Tao, Z.; Tice, M.; et al. GR231118 (1229U91) and other analogues of the C-terminus of neuropeptide Y are potent neuropeptide Y Y1 receptor antagonists and neuropeptide Y Y4 receptor agonists. *Eur. J. Pharmacol.* **1998**, *349*, 97–105. [[CrossRef](#)]
96. Ziemek, R.; Schneider, E.; Kraus, A.; Cabrele, C.; Beck-Sickingler, A.G.; Bernhardt, G.; Buschauer, A. Determination of Affinity and Activity of Ligands at the Human Neuropeptide Y Y4 Receptor by Flow Cytometry and Aequorin Luminescence. *J. Recept. Signal. Transduct. Res.* **2007**, *27*, 217–233. [[CrossRef](#)]
97. Gehlert, D.R. Neuropeptide Y (NPY) and its Receptors. In *Encyclopedia of Neuroscience*; Squire, L.R., Ed.; Academic Press: Cambridge, MA, USA, 2009; pp. 837–842. [[CrossRef](#)]
98. Campbell, R.E.; Smith, M.S.; Allen, S.E.; Grayson, B.E.; Ffrench-Mullen, J.; Grove, K.L. Orexin Neurons Express a Functional Pancreatic Polypeptide Y4 Receptor. *J. Neurosci.* **2003**, *23*, 1487–1497. [[CrossRef](#)] [[PubMed](#)]
99. Horvath, T.L.; Pu, S.; Dube, M.G.; Diano, S.; Kalra, S.P. A GABA-neuropeptide Y (NPY) interplay in LH release. *Peptides* **2001**, *22*, 473–481. [[CrossRef](#)]
100. Santos-Carvalho, A.; Elvas, F.; Álvaro, A.R.; Ambrósio, A.F.; Cavadas, C. Neuropeptide Y receptors activation protects rat retinal neural cells against necrotic and apoptotic cell death induced by glutamate. *Cell Death Dis.* **2013**, *4*, e636. [[CrossRef](#)] [[PubMed](#)]
101. Parker, E.M.; Balasubramaniam, A.; Guzzi, M.; Mullins, D.E.; Salisbury, B.G.; Sheriff, S.; Witten, M.B.; Hwa, J.J. [D-Trp(34)] neuropeptide Y is a potent and selective neuropeptide Y Y(5) receptor agonist with dramatic effects on food intake. *Peptides* **2000**, *21*, 393–399. [[CrossRef](#)]
102. Cabrele, C.; Langer, M.; Bader, R.; Wieland, H.A.; Doods, H.N.; Zerbe, O.; Beck-Sickingler, A.G. The First Selective Agonist for the Neuropeptide YY5 Receptor Increases Food Intake in Rats. *J. Biol. Chem.* **2000**, *275*, 36043–36048. [[CrossRef](#)]
103. Cabrele, C.; Beck-Sickingler, A.G. Molecular Characterization of the Ligand – Receptor Interaction of the Neuropeptide Y Family. *J. Pept. Sci.* **2000**, *6*, 97–122. [[CrossRef](#)]
104. Dumont, Y.; Thakur, M.; Beck-Sickingler, A.; Fournier, A.; Quirion, R. Development and characterization of a highly selective neuropeptide Y Y5 receptor agonist radioligand: [125I][hPP(1-17), Ala31, Aib32]NPY. *Br. J. Pharmacol.* **2003**, *139*, 1360–1368. [[CrossRef](#)]
105. Dumont, Y.; Thakur, M.; Beck-Sickingler, A.; Fournier, A.; Quirion, R. Characterization of a new neuropeptide Y Y5 agonist radioligand: [125I][cPP(1–7), NPY(19–23), Ala31, Aib32, Gln34]hPP. *Neuropeptides* **2004**, *38*, 163–174. [[CrossRef](#)]
106. Balasubramaniam, A.; Sheriff, S.; Zhai, W.; Chance, W.T. Bis(31/31')[[Cys31, Nva34]NPY(27–36)-NH₂]: A neuropeptide Y (NPY) Y5 receptor selective agonist with a latent stimulatory effect on food intake in rats. *Peptides* **2002**, *23*, 1485–1490. [[CrossRef](#)]
107. Criscione, L.; Rigollier, P.; Batzl-Hartmann, C.; Rüeger, H.; Stricker-Krongrad, A.; Wyss, P.; Brunner, L.; Whitebread, S.; Yamaguchi, Y.; Gerald, C.; et al. Food Intake in Free-feeding and Energy-deprived Lean Rats Is Mediated by the Neuropeptide Y5 Receptor. *J. Clin. Investig.* **1998**, *102*, 2136–2145. [[CrossRef](#)]
108. Kanatani, A.; Ishihara, A.; Iwaasa, H.; Nakamura, K.; Okamoto, O.; Hidaka, M.; Ito, J.; Fukuroda, T.; MacNeil, D.J.; Van der Ploeg, L.H.T.; et al. L-152,804: Orally Active and Selective Neuropeptide Y Y5 Receptor Antagonist. *Biochem. Biophys. Res. Commun.* **2000**, *272*, 169–173. [[CrossRef](#)] [[PubMed](#)]
109. Kakui, N.; Tanaka, J.; Tabata, Y.; Asai, K.; Masuda, N.; Miyara, T.; Nakatani, Y.; Ohsawa, F.; Nishikawa, N.; Sugai, M.; et al. Pharmacological Characterization and Feeding-Suppressive Property of FMS586 [3-(5,6,7,8-Tetrahydro-9-isopropylcarbazol-3-yl)-1-methyl-1-(2-pyridin-4-yl-ethyl)-urea Hydrochloride], a Novel, Selective, and Orally Active Antagonist for Neuropeptide Y Y5 Receptor. *J. Pharmacol. Exp. Ther.* **2006**, *317*, 562–570. [[CrossRef](#)] [[PubMed](#)]
110. Walker, M.W.; Wolinsky, T.D.; Jubian, V.; Chandrasena, G.; Zhong, H.; Huang, X.; Miller, S.; Hegde, L.G.; Marsteller, D.A.; Marzabadi, M.R.; et al. The Novel Neuropeptide Y Y5 Receptor Antagonist Lu AA33810 [N-[[trans-4-[(4,5-Dihydro[1]benzothiepin[5,4-d]thiazol-2-yl)amino]cyclohexyl]methyl]-methanesulfonamide] Exerts Anxiolytic- and Antidepressant-Like Effects in Rat Models of Stress Sensitivity. *J. Pharmacol. Exp. Ther.* **2009**, *328*, 900–911. [[CrossRef](#)] [[PubMed](#)]

111. Della-Zuana, O.; Revereault, L.; Beck-Sickinger, A.; Monge, A.; Caignard, D.-H.; Fauchère, J.-L.; Henlin, J.-M.; Audinot, V.; Boutin, J.A.; Chamorro, S.; et al. A potent and selective NPY Y5 antagonist reduces food intake but not through blockade of the NPY Y5 receptor. *Int. J. Obes. Relat. Metab. Disord.* **2004**, *28*, 628–639. [[CrossRef](#)] [[PubMed](#)]
112. Block, M.H.; Boyer, S.; Brailsford, W.; Brittain, D.R.; Carroll, D.; Chapman, S.; Clarke, D.S.; Donald, C.S.; Foote, K.M.; Godfrey, L.; et al. Discovery and Optimization of a Series of Carbazole Ureas as NPY5 Antagonists for the Treatment of Obesity. *J. Med. Chem.* **2002**, *45*, 3509–3523. [[CrossRef](#)]
113. Satoh, Y.; Hatorib, C.; Ito, H. Novel Potent Antagonists of Human Neuropeptide Y-Y5 Receptor. Part 4: Tetrahydrodiazabenzazulene Derivatives. *Bioorg. Med. Chem. Lett.* **2002**, *12*, 1009–1011. [[CrossRef](#)]
114. Daniels, A.J.; Grizzle, M.K.; Wiard, R.P.; Matthews, J.E.; Heyer, D. Food intake inhibition and reduction in body weight gain in lean and obese rodents treated with GW438014A, a potent and selective NPY-Y5 receptor antagonist. *Regul. Pept.* **2002**, *106*, 47–54. [[CrossRef](#)]
115. Islam, I.; Dhanoa, D.; Finn, J.; Du, P.; Walker, M.W.; Salon, J.A.; Zhang, J.; Gluchowski, C. Discovery of Potent and Selective Small Molecule NPY Y5 Receptor Antagonists. *Bioorg. Med. Chem. Lett.* **2002**, *12*, 1767–1769. [[CrossRef](#)]
116. Oda, S.; Manaka, K.; Kakiya, K.; Hozumi, Y.; Fukui, Y.; Omura, S.; Kurashita, M.; Nishiwaki, M.; Takeuchi, Y.; Kitamura, H. Development of an Optimized Synthetic and Purification Process of S-2367 (Velneperit), a Novel Neuropeptide Y (NPY) Y5 Receptor Antagonist. *Org. Process. Res. Dev.* **2015**, *19*, 531–536. [[CrossRef](#)]
117. Mullins, D.; Adham, N.; Hesk, D.; Wu, Y.; Kelly, J.; Huang, Y.; Guzzi, M.; Zhang, X.; McCombie, S.; Stamford, A.; et al. Identification and characterization of pseudoirreversible nonpeptide antagonists of the neuropeptide Y Y5 receptor and development of a novel Y5-selective radioligand. *Eur. J. Pharmacol.* **2008**, *601*, 1–7. [[CrossRef](#)]
118. Nichol, K.A.; Morey, A.; Couzens, M.H.; Shine, J.; Herzog, H.; Cunningham, A.M. Conservation of Expression of Neuropeptide Y5 Receptor between Human and Rat Hypothalamus and Limbic Regions Suggests an Integral Role in Central Neuroendocrine Control. *J. Neurosci.* **1999**, *19*, 10295–10304. [[CrossRef](#)] [[PubMed](#)]
119. Matsumoto, M.; Nomura, T.; Momose, K.; Ikeda, Y.; Kondou, Y.; Akiho, H.; Togami, J.; Kimura, Y.; Okada, M.; Yamaguchi, T. Inactivation of a Novel Neuropeptide Y/Peptide YY Receptor Gene in Primate Species. *J. Biol. Chem.* **1996**, *271*, 27217–27220. [[CrossRef](#)] [[PubMed](#)]
120. Gregor, P.; Millham, M.L.; Feng, Y.; DeCarr, L.B.; McCaleb, M.L.; Cornfield, L.J. Cloning and characterization of a novel receptor to pancreatic polypeptide, a member of the neuropeptide Y receptor family. *FEBS Lett.* **1996**, *381*, 58–62. [[CrossRef](#)]
121. Khor, E.-C.; Yulyaningsih, E.; Driessler, F.; Kovačić, N.; Wee, N.K.Y.; Kulkarni, R.N.; Lee, N.J.; Enriquez, R.F.; Xu, J.; Zhang, L.; et al. The y6 receptor suppresses bone resorption and stimulates bone formation in mice via a suprachiasmatic nucleus relay. *Bone* **2016**, *84*, 139–147. [[CrossRef](#)] [[PubMed](#)]
122. Patel, S.; Gibson, R. In vivo site-directed radiotracers: A mini-review. *Nucl. Med. Biol.* **2008**, *35*, 805–815. [[CrossRef](#)] [[PubMed](#)]
123. Kameda, M.; Ando, M.; Nakama, C.; Kobayashi, K.; Kawamoto, H.; Ito, S.; Suzuki, T.; Tani, T.; Ozaki, S.; Tokita, S.; et al. Synthesis and evaluation of a series of 2,4-diaminopyridine derivatives as potential positron emission tomography tracers for neuropeptide Y Y1 receptors. *Bioorg. Med. Chem. Lett.* **2009**, *19*, 5124–5127. [[CrossRef](#)]
124. Hostetler, E.D.; Sanabria-Bohórquez, S.; Fan, H.; Zeng, Z.; Gantert, L.; Williams, M.; Miller, P.; O'Malley, S.; Kameda, M.; Ando, M.; et al. Synthesis, characterization, and monkey positron emission tomography (PET) studies of [¹⁸F]Y1-973, a PET tracer for the neuropeptide Y Y1 receptor. *NeuroImage* **2011**, *54*, 2635–2642. [[CrossRef](#)]
125. Reubi, J.C.; Gugger, M.; Waser, B.; Schaer, J.-C. Y1-Mediated Effect of Neuropeptide Y in Cancer: Breast Carcinomas as Targets. *Cancer Res.* **2001**, *61*, 4636–4641.
126. Hofmann, S.; Maschauer, S.; Kuwert, T.; Beck-Sickinger, A.G.; Prante, O. Synthesis and in Vitro and in Vivo Evaluation of an ¹⁸F-Labeled Neuropeptide Y Analogue for Imaging of Breast Cancer by PET. *Mol. Pharm.* **2015**, *12*, 1121–1130. [[CrossRef](#)]
127. Keller, M.; Maschauer, S.; Brennauer, A.; Tripal, P.; Koglin, N.; Dittrich, R.; Bernhardt, G.; Kuwert, T.; Wester, H.-J.; Buschauer, A.; et al. Prototypic ¹⁸F-Labeled Argininamide-Type Neuropeptide Y Y1R Antagonists as Tracers for PET Imaging of Mammary Carcinoma. *ACS Med. Chem. Lett.* **2017**, *8*, 304–309. [[CrossRef](#)]
128. Maschauer, S.; Ott, J.J.; Bernhardt, G.; Kuwert, T.; Keller, M.; Prante, O. ¹⁸F-labelled triazolyl-linked argininamides targeting the neuropeptide Y Y1R for PET imaging of mammary carcinoma. *Sci. Rep.* **2019**, *9*, 12990. [[CrossRef](#)] [[PubMed](#)]
129. Maschauer, S.; Haubner, R.; Kuwert, T.; Prante, O. ¹⁸F-Glyco-RGD Peptides for PET Imaging of Integrin Expression: Efficient Radiosynthesis by Click Chemistry and Modulation of Biodistribution by Glycosylation. *Mol. Pharm.* **2014**, *11*, 505–515. [[CrossRef](#)] [[PubMed](#)]
130. Kawamura, K.; Mori, W.; Fujinaga, M.; Yamasaki, T.; Zhang, Y.; Wakizaka, H.; Hatori, A.; Xie, L.; Kumata, K.; Ohkubo, T.; et al. Radiosynthesis and in vivo evaluation of ¹¹C-labeled BMS-193885 and its desmethyl analog as PET tracers for neuropeptide Y1 receptors. *EJNMMI Radiopharm. Chem.* **2019**, *4*, 1–13. [[CrossRef](#)] [[PubMed](#)]
131. Antal-Zimanyi, I.; Bruce, M.A.; LeBoulluec, K.L.; Iben, L.G.; Mattson, G.K.; McGovern, R.T.; Hogan, J.B.; Leahy, C.L.; Flowers, S.C.; Stanley, J.A.; et al. Pharmacological characterization and appetite suppressive properties of BMS-193885, a novel and selective neuropeptide Y1 receptor antagonist. *Eur. J. Pharmacol.* **2008**, *590*, 224–232. [[CrossRef](#)]
132. Vall-Sagarra, A.; Litau, S.; Decristoforo, C.; Wängler, B.; Schirmacher, R.; Fricker, G.; Wängler, C. Design, Synthesis, In Vitro, and Initial In Vivo Evaluation of Heterobivalent Peptidic Ligands Targeting Both NPY(Y1)- and GRP-Receptors- An Improvement for Breast Cancer Imaging? *Pharmaceuticals* **2018**, *11*, 65. [[CrossRef](#)] [[PubMed](#)]

133. Krieger, K.; Wängler, B.; Schirmmayer, R.; Wängler, C. Identification of a Suitable Peptidic Molecular Platform for the Development of NPY(Y1)R-Specific Imaging Agents. *ChemMedChem* **2020**, *15*, 1652–1660. [[CrossRef](#)]
134. Cardoso, M.E.; Tejería, E.; Zirbesegger, K.; Savio, E.; Terán, M.; Rey Ríos, A.M. Development and characterization of two novel ⁶⁸Ga-labelled neuropeptide Y short analogues with potential application in breast cancer imaging. *Chem. Biol. Drug Des.* **2021**, *98*, 182–191. [[CrossRef](#)]
135. Winterdahl, M.; Audrain, H.; Landau, A.M.; Smith, D.F.; Bonaventure, P.; Shoblock, J.R.; Carruthers, N.; Swanson, D.; Bender, D. PET Brain Imaging of Neuropeptide Y2 Receptors Using N-11C-Methyl-JNJ-31020028 in Pigs. *J. Nucl. Med.* **2014**, *55*, 635–639. [[CrossRef](#)]
136. Andersen, T.L.; Friis, S.D.; Audrain, H.; Nordeman, P.; Antoni, G.; Skrydstrup, T. Efficient 11C-Carbonylation of Isolated Aryl Palladium Complexes for PET: Application to Challenging Radiopharmaceutical Synthesis. *J. Am. Chem. Soc.* **2015**, *137*, 1548–1555. [[CrossRef](#)]
137. Hostetler, E.; Sanabria, S.; Krause, S.; Ryan, C.; Francis, B.; Eng, W.S.; Hargreaves, R.; Burns, D. Neuropeptide-Y Y5 (NPY5) receptor: Occupancy studies in Rhesus monkey using a novel NPY5 PET tracer. *Neuroimage* **2006**, *31*, T16. [[CrossRef](#)]
138. Takahashi, H.; Haga, Y.; Shibata, T.; Nonoshita, K.; Sakamoto, T.; Moriya, M.; Ohe, T.; Chiba, M.; Mitobe, Y.; Kitazawa, H.; et al. Identification of positron emission tomography ligands for NPY Y5 receptors in the brain. *Bioorg. Med. Chem. Lett.* **2009**, *19*, 5436–5439. [[CrossRef](#)] [[PubMed](#)]
139. Kealey, S.; Plisson, C.; Collier, T.L.; Long, N.J.; Husbands, S.M.; Martarello, L.; Gee, A.D. Microfluidic reactions using [11C]carbon monoxide solutions for the synthesis of a positron emission tomography radiotracer. *Org. Biomol. Chem.* **2011**, *9*, 3313–3319. [[CrossRef](#)] [[PubMed](#)]
140. Kumar, J.S.D.; Walker, M.; Packiarajan, M.; Jubian, V.; Prabhakaran, J.; Chandrasena, G.; Pratap, M.; Parsey, R.V.; Mann, J.J. Radiosynthesis and in Vivo Evaluation of Neuropeptide Y5 Receptor (NPY5R) PET Tracers. *ACS Chem. Neurosci.* **2016**, *7*, 540–545. [[CrossRef](#)] [[PubMed](#)]